MAGNETIC BUBBLE MATERIALS

Jerry W. Moody, et al

Monsanto Research Corporation

Prepared for:

Advanced Research Projects Agency

11 August 1973

MRC-SL-386

FINAL REPORT

MAGNETIC BUBBLE MATERIALS

Monsanto Research Corporation
St. Louis, Missouri 63166

Jerry W. Moody, Robert M. Sandfort, Roger W. Shaw
Michael C. Willson, Joseph T. Cheng, and Richard J. Janowiecki

Contract No. DAAH01-72-C-1098

ARPA Support Office
Research, Development, Engineering,
and Missile Systems Laboratory
U.S. Army Missile Command
Redstone Arsenal, Alabama

Sponsored by:
Advanced Research Projects Agency
ARPA Order Nr. 1999

UNCLASSIFIED

Security Classification

DOCUMENT CONTROL DATA - R & D

(Security classification of title, body of abstract and indexing annotation must be entered when the overall report is classified)

1 ORIGINATING ACTIVITY *(Corporate author)*

Monsanto Research Corporation
800 North Lindbergh Boulevard
St. Louis, Missouri 63166

2a. REPORT SECURITY CLASSIFICATION

UNCLASSIFIED

2b. GROUP

3 REPORT TITLE

MAGNETIC BUBBLE MATERIALS

4 DESCRIPTIVE NOTES *(Type of report and inclusive dates)*

Final Report, 11 January-11 July 1973

5 AUTHOR(S) *(First name, middle initial, last name)*

J. W. Moody, Robert M. Sandfort, Roger W. Shaw, et al.

6 REPORT DATE	7a. TOTAL NO. OF PAGES	7b. NO. OF REFS
20 September 1973	54 69	28

8a. CONTRACT OR GRANT NO.	9a. ORIGINATOR'S REPORT NUMBER(S)
DAAHO1-72-C-1098	
b. PROJECT NO ARPA Order No. 1999	MRC-SL-386
c.	9b. OTHER REPORT NO(S) *(Any other numbers that may be assigned this report)*
d.	

10 DISTRIBUTION STATEMENT

Distribution of this document unlimited

11 SUPPLEMENTARY NOTES	12. SPONSORING MILITARY ACTIVITY
	Advanced Research Project Agency Washington, D.C.

13 ABSTRACT

The Czochralski growth of defect-free, non-magnetic garnet crystals and the preparation of epitaxial magnetic bubble garnet films by liquid phase epitaxy (LPE) and arc-plasma spraying (APS) were investigated. Two garnet systems, Eu-Yb-Y and Sm-Y, were identified as being of particular practical interest. These garnets exhibit reasonable mobilities, satisfactory quality factors, and good temperature stability. Device-quality films can be deposited by LPE from $PbO-B_2O_3$ solution on (111) GGG substrates. Methods were developed for growing epitaxial garnet films by APS. However, the films were usually contaminated with crystallites of orthoferrite, hematite, magnetoplumbite or other phases. Low-defect-density films were not prepared and the elimination of unwanted phases by compositional control appears to be a formidable problem. All recent developments indicate that the LPE "dipping" growth of garnet films is a commercially viable process. Core-free single crystals of GGG with defect densities of less than 5 per cm^2 can be grown readily by the Czochralski method. Such crystals, up to 38 mm in diameter, are now available commercially.

DD FORM 1 NOV 65 1473

UNCLASSIFIED

Security Classification

14 KEY WORDS	LINK A		LINK B		LINK C	
	ROLE	WT	ROLE	WT	ROLE	WT
Magnetic bubble materials						
Magnetic garnets						
Gadolinium gallium garnets						
Crystal growth						
Liquid phase epitaxy						
Chemical vapor deposition						
Arc plasma spray						
Substrate preparation						
Rare-earth iron garnets						

FINAL REPORT

MAGNETIC BUBBLE MATERIALS

Monsanto Research Corporation
St. Louis, Missouri 63166

Jerry W. Moody, Robert M. Sandfort, Roger W. Shaw,
Michael C. Willson, Joseph T. Cheng, and Richard J. Janowiecki

August 11, 1973

Contract No. DAAH01-72-C-1098

Distribution of this document is unlimited

ARPA Support Office
Research, Development, Engineering
and Missile Systems Laboratory
U.S. Army Missile Command
Redstone Arsenal, Alabama

Sponsored by:
Advanced Research Projects Agency
ARPA Order No. 1999

SUMMARY

This is the final report on the project "Magnetic Bubble Materials, Phase II," Contract No. DAAH01-72-C-1098. It covers in detail the work performed from January 11, 1973 through July 11, 1973. The Czochralski growth of defect-free non-magnetic garnet crystals, the preparation of epitaxial magnetic bubble garnet films by liquid phase epitaxy (LPE) and arc-plasma spraying (APS) were investigated. References to earlier work are included for the sake of completeness.

Two garnet systems, Eu-Yb-Y and Sm-Y were identified as being of particular practical interest. These garnets exhibit reasonable mobilities, satisfactory quality factors and good temperature stability. Device quality films can be deposited by LPE from $PbO-B_2O_3$ solution on (111) GGG substrates.

Methods were developed for growing epitaxial garnet films by APS. However, the films were usually contaminated with crystallites of orthoferrite, hematite, magnetoplumbite or other phases. Low defect density films were not prepared and the elimination of unwanted phases by compositional control appears to be a formidable problem.

All recent developments indicate that the LPE "dipping" growth of garnet films is a commercially viable process. This method is now used almost exclusively by workers in the field.

Core-free single crystals of GGG with defect densities of less than 5 per cm^2 can be grown readily by the Czochralski method. Such crystals, up to 38 mm in diameter, are now available from commercial vendors.

TABLE OF CONTENTS

LIST OF FIGURES

LIST OF TABLES

1.0 INTRODUCTION

This is the final report on the project "Magnetic Bubble Materials - Phase II", Contract No. DAAH01-72-C-1098. This project was a continuation of work performed under Contract No. DAAH01-72-C-0490. The primary objective of this work was to fulfill a need for a supply of reproducible, low defect, high quality magnetic bubble materials to support the device work of various DOD agencies who are investigating the application of these materials for end uses of importance to national security. The work has involved development of methods to grow high quality bulk crystals for use as substrates, development of substrate polishing and preparation procedures, studies of epitaxial film growth by three different methods: liquid phase epitaxy (LPE), chemical vapor deposition (CVD), and arc-plasma spraying (APS); and development of methods to fully characterize bubble domain materials.

Two reports[1, 2] have been issued previously which presented in detail the preparation of garnet films and crystals, and the progress of bubble materials technology. Two reports[3, 4] covering characterization techniques have been issued also. One,[4] a comprehensive, critical survey of characterization procedures, has been widely accepted as a valuable aid by workers in the field.

This report covers the work accomplished from February 11, 1973 through July 11, 1973. Specifically, it discusses the LPE growth of films of the Eu-Yb-Y and Sm-Y systems and the preparation of garnet films by APS. In addition, a section is devoted to up-dating characterization

procedures. Finally, the report is concluded with a brief survey of bubble materials technology and recommendations for future work.

2.0 CHARACTERIZATION

The majority of the methods employed in the characterization of the garnet films grown under this contract have been dealt with in detail in earlier reports.[1, 3, 4] The following brief discussion is thus intended only to summarize these methods and present relevant detail where new techniques have been instituted since those reports were prepared.

2.1 Film Thickness

The thickness of the magnetic garnet films has been measured using optical interference of reflected light[4]. Thickness uniformity also has involved the use of optical interference, in this case in the form of a contour map caused by interference of monochromatic light reflected from the front and back of the film.[4]

2.2 Defect Detection and Location

Defects which impede domain motion are readily observed using a polarizing microscope and an alternating bias field sufficient to cause most of the strip domains to move[4]. Experience at Monsanto has indicated that this method, when properly employed, is sufficiently sensitive to detect all defects likely to cause difficulties in devices of present design.

2.3 Characteristic Length and Domain Dimensions

Where possible, domain dimensions have been measured on parallel strip domain patterns in order to improve accuracy. This includes the determination of characteristic length from the film thickness and strip domain period.[4, 5, 6] Bubble domain diameters are routinely measured at the stability limits but such results are of more limited accuracy.

2.4 Saturation Magnetization and Magnetic Fields

The saturation magnetization was derived from the measurement of the highest bias field at which normal bubbles are stable (the collapse field) combined with a knowledge of the zero field strip domain width and the thickness. The theory required has been worked out by Thiele (7), and Fowlis and Copeland (5) with useful graphical results in several places. (4) A calibrated bias coil mounted on the stage of a polarizing microscope served as source for most of the magnetic fields needed in the work. For situations in which the sample was inaccessible, as in a variable temperature stage, the saturation magnetization was usually derived from an optical hysteresis loop. (4, 6)

2.5 Coercivity

A measure of sample coercivity results from determination of the polarized light intensity modulation resulting from several amplitudes of bias field modulation. The plot of light modulation vs. field modulation amplitudes yields an approximately linear relationship which extrapolates, for zero light modulation, to a finite field amplitude--the coercivity field. (4) This technique, while a worthwhile relative measure, usually yields values smaller than the half-width of the complete hysteresis loop and so has little absolute meaning. Experimentally, samples of coercivity greater than approximately 0.5 Oe show measurably degraded characteristics in devices.

2.6 Anisotropy

The measurement of magnetic anisotropy field, H_A, by magneto-optical techniques, was just under development at the time of preparation of ref. 4 . The recent papers of Shumate, et al. (8, 9) place this measure-

ment on a much better footing than it was at that time. In particular they form the basis for a technique proposed by Josephs[10] and now used almost exclusively in this laboratory. In this method a large field is applied in the plane of the film, rotating the magnetization into this plane. An alternating bias field normal to the film still yields a small optical modulation proportional to the susceptibility in the normal direction. For fields H greater than $H_A - 4\pi M_s$, this susceptibility is given by $X = M_s/(H + 4\pi M_s - H_A)$. Thus a plot of X^{-1} (or the proportional inverse light modulation amplitude) versus H yields a linear relationship with an intercept at $X^{-1} = 0$ of $H = H_A - 4\pi M_s$. This linear relationship is quite consistently observed when the proper alignment of the sample has been established. The resulting values of H_A are accurate to roughly $\pm 10\%$.

It should be noted that the method outlined in ref. 4 (the assignment of the low field shoulder as $H_A - 4\pi M_s$) is in error. This shoulder is, to within $\sim 10\%$, equal to H_A but its interpretation is not on as sound theoretical footing as is the method outlined above, so that the latter has been adopted as standard.

2.7 Temperature Effects

The means of measuring the Neel Temperature using a microscope hot stage and optical detection has been discussed previously.[4] Compensation temperatures were measured in somewhat similar fashion where, however, no microscope was used. Instead, light was conducted to the sample by means of a fiber optic "light pipe", then polarized, sent through the sample, analyzed, and brought out to a photomultiplier via another light

pipe. The sample was in a coil within a Dewar vessel where its temperature was adjusted by means of location in the Dewar and a heater coil. The coil provided an alternating bias field and the synchronous optical signal served as a measure of the state of the sample. At compensation the phase of the optical signal changes by 180°, generally accompanied by a range of high coercivity and therefore small or zero signal. A substantial drive field was applied to keep this range $\lesssim$ 10°C and the compensation temperature was taken as the center of this range.

Determination of temperature effects on characteristic length, saturation magnetization, and mobility near room temperature involved the use of a thermoelectric variable temperature stage in the microscope. Such an addition made these measurements possible over a range from -10 to +60°C.

3.0 LIQUID PHASE EPITAXY

3.1 Review

Six different film compositions were supplied to the Sponsor during the first phase of this program:

1. $Eu_{0.6}Er_{2.4}Fe_{4.4}Ga_{0.6}O_{12}$
2. $Gd_{0.8}Er_{2.2}Fe_{4.6}Ga_{0.4}O_{12}$
3. $Gd_{0.5}Y_{2.5}Fe_4Ga_1O_{12}$
4. $Gd_1Yb_{0.9}Y_{1.1}Fe_{4.2}Ga_{0.8}O_{12}$
5. $Gd_{0.44}La_{0.44}Y_{2.52}Fe_4Ga_1O_{12}$
6. $Gd_{1.1}Tm_{0.9}Y_1Fe_{4.3}Ga_{0.7}O_{12}$

Although all these compositions were tailored to support stable 5 - 7 μm bubble domains, they exhibit a wide range and variety of magnetic properties. The anisotropy of compositions 1 and 2 is primarily growth induced; that of composition 3 is stress-induced, while that of compositions 4, 5, and 6 is probably both growth- and stress-induced. The magnitude of the anisotropies range from about 500 Oe (for composition 3) to 3800 Oe (composition 1) while domain mobilities range from less than 100 cm/sec/Oe (composition 1) to over 600 cm/sec/Oe (composition 4).

Because of their range of properties these first compositions were valuable for basic property studies and preliminary device work. However, none of the compositions possessed the combination of high mobility and temperature stability that is required for a practical device. Therefore, during the second phase of the program attention was directed toward developing compositions with adequate temperature stability which also have

the desirable features of several of the compositions in the above list. The guidelines for compositional development and the requirements for temperature stability were discussed in detail in the Semi-Annual Technical Report.[2] Briefly, the discussion pointed out the potentialities inherent in the mixed Eu-Y, Sm-Y, and Nd-Y magnetic garnets, and these systems were investigated during the second phase of the program. Since Eu exhibits little or no angular momentum and $Eu_3Fe_5O_{12}$ has no compensation point, the Eu-Y system was of particular interest. Magnetic garnet films of the Eu-Y system were supplied to the Sponsor early in this program. More recently, Sm-Y garnets were prepared and supplied to the Sponsor. In addition small additions of Yb were introduced into the Eu-Y garnets to improve domain wall mobility characteristics and samples of these materials were also supplied to the Sponsor. The Nd-Y system was also investigated but, in this case, the magnetization was found to be in the plane of the film.

The preparation and properties of all these magnetic films are described in this section of the report. Some of this work was presented previously in the Semi-Annual Technical Report.[2] It is repeated here for the sake of completeness.

3.2 Experimental

The apparatus and methods used to grow magnetic garnet films by LPE have been described previously.[1, 2] The magnetic bubble films were grown by the isothermal dipping method[11] from $PbO-B_2O_3$ solutions. The films were grown both statically and with rotation. However, during this

phase of the program most films were grown horizontally at a rotation rate of 200 rpm to ensure thickness uniformity.

The work was directed toward developing solution compositions in which could be grown magnetic films which supported stable 5 - 7 μm bubbles. In practice, a series of films with constant rare earth ratio but with varying Ga content was prepared by adding appropriate increments of Ga_2O_3 to the solution. The magnetic properties of the films were measured and the films were examined for evidence of excessive tension (cracking) or compression (faceting). Those solution compositions which produced sound, smooth films having the desired magnetic properties were then used to grow films for delivery to the Sponsor.

All films were deposited on Syton-polished, (111) GGG substrates. The thickness of the films ranged from about 3 to 10 μm. The thickness uniformity of films grown with axial rotation was about ± 1 percent.

3.3 The Eu-Y-Yb System

3.3.1 Introduction

The preparation of $Eu_2Y_1Fe_{5-x}Al_xO_{12}$ and $Eu_{0.6}Y_{2.4}Fe_{5-x}Ga_xO_{12}$ films were described in the Semi-Annual Technical Report.[2] The high Eu, Al-containing films were characterized by high coercivities (≈0.5 Oe) and low domain wall mobilities (<100 cm/sec/Oe in zero in-plane field). The low Eu, Ga-containing films also exhibited relatively high coercivities (≈0.3 Oe) and domain wall mobilities of about 200 cm/sec/Oe in zero in-plane field. This value is about the minimum acceptable mobility for magnetic bubble devices. Bonner, et al.[12] found that small additions of Yb would reduce the dynamic

instabilities which give rise to velocity saturation at device magnitude drive fields and concomitant low mobility values in Eu-Y garnet films. In other work at Monsanto,[13] the effect of Yb additions to the low Eu, Ga-containing garnet films had been investigated in detail. Because of wide variability from sample to sample, the dependence of mobility on Yb content was not clear-cut; however, a definite improvement was obtained. The results suggested that a maximum mobility, in zero bias field, of about 600 cm/sec/Oe was attained with about 0.2 Yb ion molecule. For in-plane fields of about 40 Oe, a maximum mobility of about 1500 cm/sec/Oe was attained with about 0.1 Yb ion/molecule. Therefore, an addition of about 0.15 ion molecule appeared to be a desirable Yb content. Having decided the Yb content, the Eu, Y and Ga contents were then adjusted to yield smooth, uncrazed films which supported stable 5 - 7 μm bubbles. The dependence of magnetic properties on compositions of these films as well as previously prepared Eu-Y films are presented here.

3.3.2 Properties of the Eu-Yb-Y System

3.3.2.1 Magnetization

The dependence of room temperature saturation magnetization on gallium content is shown in Fig. 1. The magnetization of other Eu-Y compositions (prepared previously) are also shown for comparison. Magnetization decreases with increasing Ga (or Al) but does not depend strongly on the concentration ratio of rare-earths.

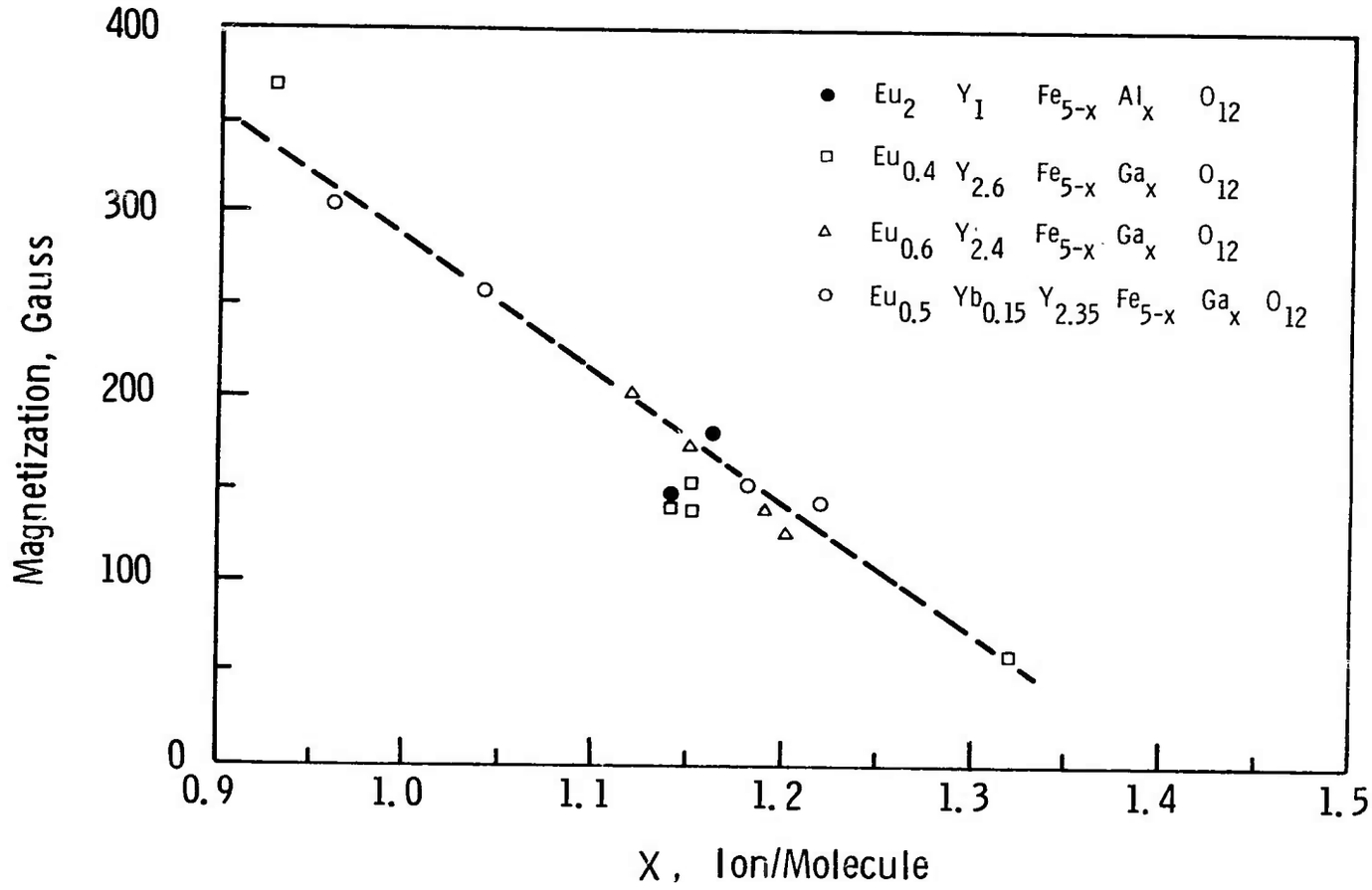

Figure 1. Magnetization vs. Gallium Content for Eu-Yb-Y Films

3.3.2.2 Characteristic Length

Characteristic length increases with Ga content as is shown in Fig. 2. It can be seen from Figs. 1 and 2 that the magnetization of films which support 5 - 7 μm bubbles is about 150 gauss and x is approximately 1.2 ion/molecule.

The average temperature coefficient of the characteristic length from 0 to 50°C for $Eu_{0.5}Yb_{0.15}Y_{2.35}Fe_{3.8}Ga_{1.2}O_{12}$ films (the composition delivered to the Sponsor) is -0.47 percent per degree.

3.3.2.3 Anisotropy

The uniaxial anisotropy field of Eu-Yb-Y films delivered to the Sponsor is about 900 Oe, which results in a quality factor of about 6 for this material. The anisotropy field is somewhat smaller than that of Yb-free, Eu-Y films grown previously (1200-1400 Oe).

Measurements of the Neel temperature reveal an interesting feature of films grown in tension which is believed to be related to the magnetic anisotropy of these garnets. In this work, the Neel temperature is measured by use of an optical hysteresigraph. (4) The signal for a "normal" sample is illustrated in curve 'a' of Fig. 3. The Neel temperature is marked by the sharp drop of the signal to zero as the wall susceptibility drops to zero at T_N. For films grown in tension, the curves display an anamolous "tail" or "peak" as is shown in curves 'b' and 'c', respectively, of Fig. 3. In these cases, the Neel temperature is taken as the point at which the signal finally reaches zero. Since this effect is found only in Eu-containing films grown in tension, it is believed to be related to a component of anisotropy, probably stress-induced, which is not perpendicular to the plane of the film. Such a stress-induced

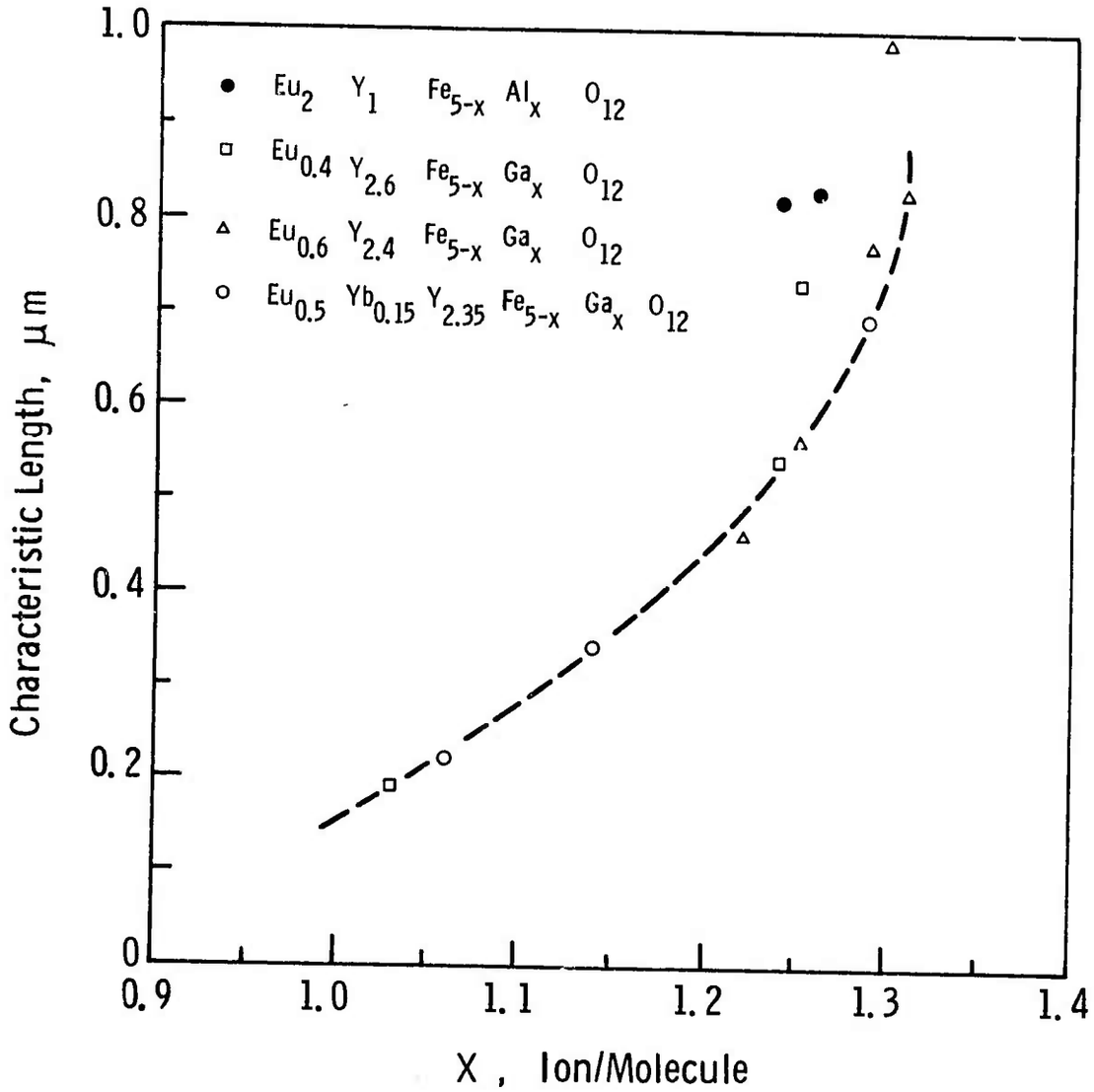

Figure 2. Characteristic Length vs. Gallium Content for Eu-Yb-Y Films

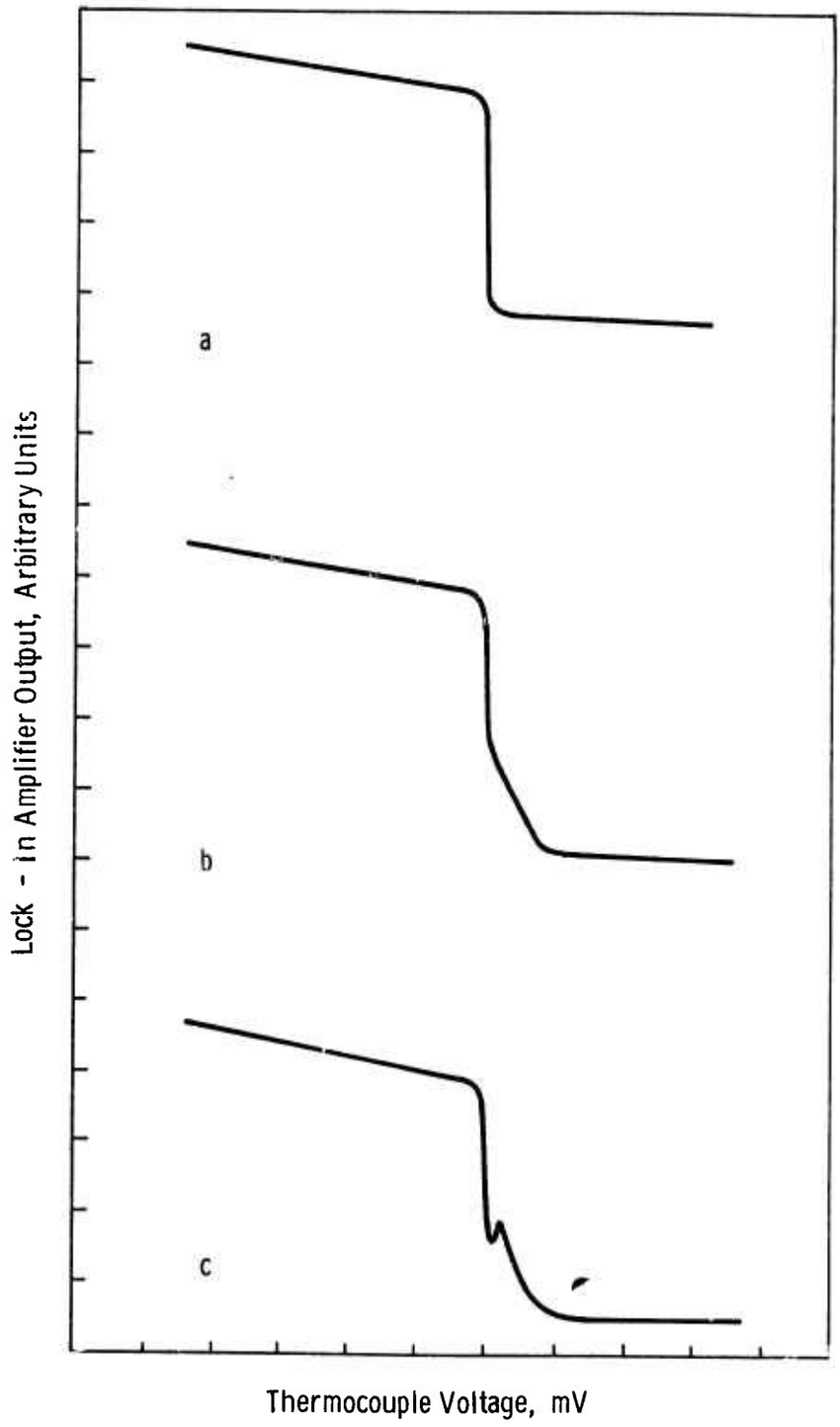

Figure 3. Optical Hysteresigraph Tracings of Neel Temperature Determinations of Eu-Yb-Y Films

component could be a result of the large, positive <100> magnetostriction coefficient of the Eu ion. If such a component is present it may affect the operating margins of bubble devices. Therefore, it is advisable to grow Eu-containing films with a close lattice match to the substrate.

3.3.2.4 Coercivity

The coercivity of the films grown for delivery was about 0.2 - 0.3 Oe. Such a relatively high value of coercivity appears to be characteristic of Eu-containing films grown in tension. Lower coercivities can be obtained by insuring a close lattice match between film and substrate.

3.3.2.5 Mobility

Mobility appears to be quite variable, both within one sample and from sample to sample of a given growth series. This effect has been previously reported by Vella-Coleiro[14] and has been thoroughly verified in the present study. While no definitive correlation with other properties has been found, certain trends are detectable.

The response of EuY garnets containing small amounts of Yb to a step change in bias field is exemplified in Fig. 4. The response at zero in-plane field is characteristic of an overdamped harmonic oscillator and is treated as discussed in reference 4. Upon application of an in-plane field, H_x, of 40 Oe or more, heavily dampled oscillations are observed which permit analysis of the type discussed in reference 15. The frequency of these oscillations generally increases as an in-plane field is applied while the decay time exhibits a tendency to decrease, as is illustrated in Fig. 5.

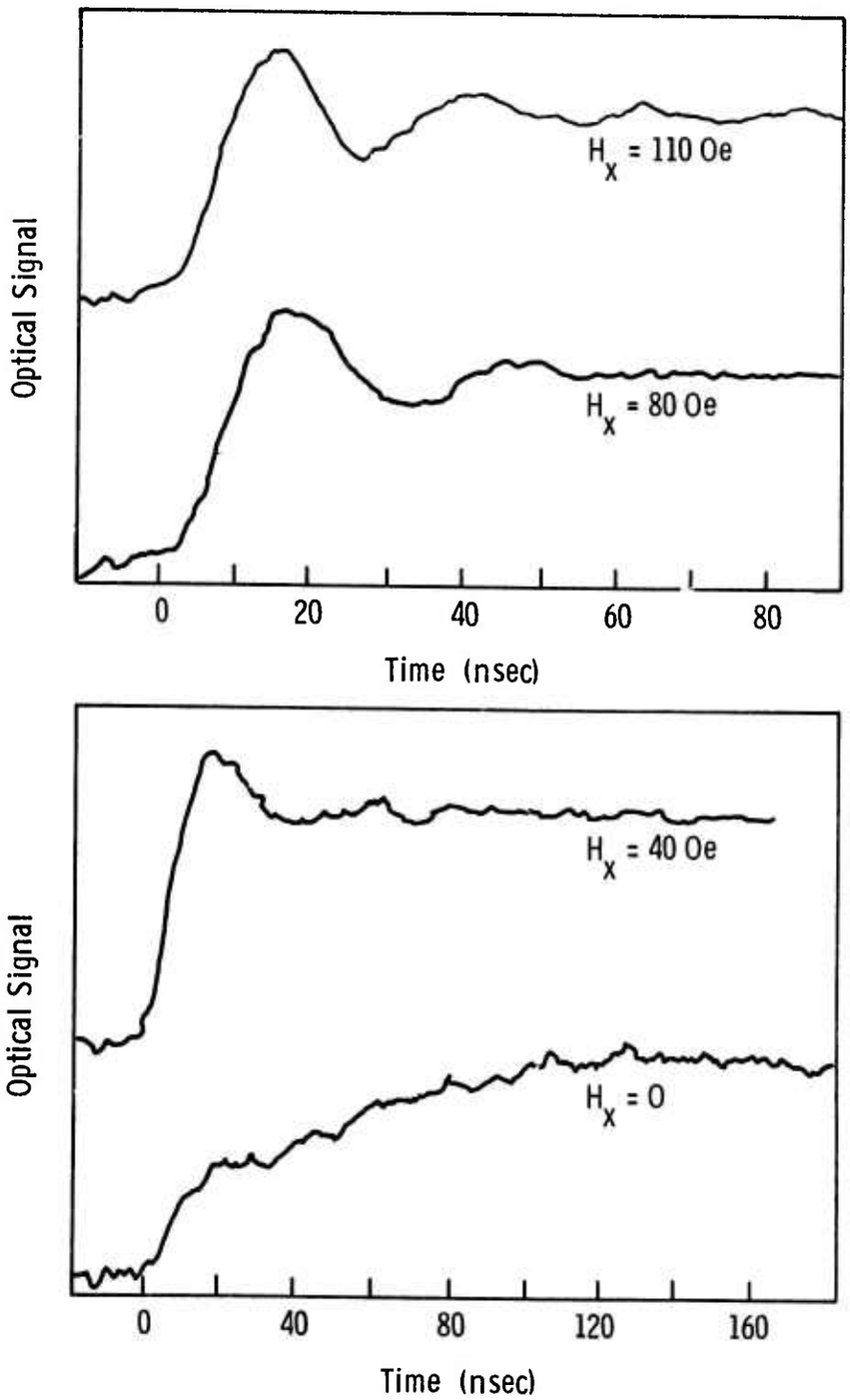

Figure 4. Optical Response of a Typical Sample of Eu-Yb-Y Garnet to a Step Rise in Bias Field at Various In-Plane Fields

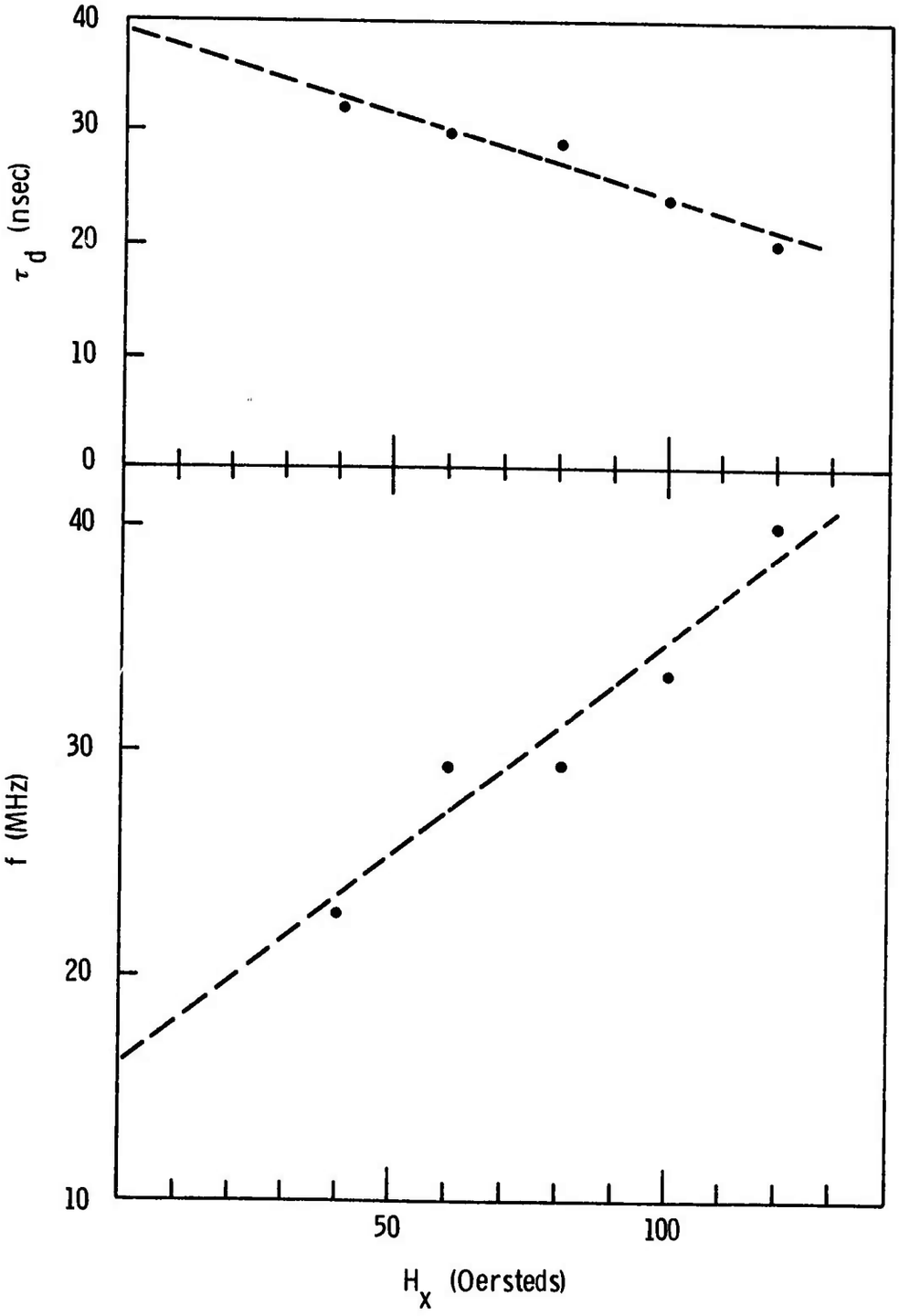

Figure 5. Natural Frequency and Decay Time vs. In-Plane Field for a Typical Sample of Eu-Yb-Y Garnet

There is a reasonably linear frequency vs. H_x characteristic which is consistently observed in all compositions in which this oscillatory behavior is observed. The internal agreement of the τ_d data must be considered largely fortuitous.

Fig. 6 illustrates the behavior of the mobility with in-plane field as determined both from the oscillatory behavior and the over-damped results, where these have been observed. The oscillatory result at $H_x = 0$ is determined for the extrapolations shown on Fig. 5. We tentatively assign the difference between these results to a suppression of turbulent motion of the wall by the in-plane field.[16] The presence of an in-plane field in a device will clearly improve the speed of the device.

The variation of mobility with temperature has not been a routine measurement in this study because of the various equipment complexities involved. It is, nonetheless, an important characteristic of any material destined for use over a significant temperature range. We have therefore recently initiated such measurements using the step field response method within a thermoelectric variable temperature stage.

Mobility was found to decrease as temperature was lowered, as is shown in Fig. 7. The wall mobility in $H_x = 0$ at -10°C ranges from 50 to 150 cm/sec/Oe. For $H_x = 33$ Oe (limited by the variable temperature apparatus) low temperature mobilities between 180 and 500 cm/sec Oe were observed, there being a definite correlation between values for $H_x = 0$ and those for $H_x = 33$ Oe.

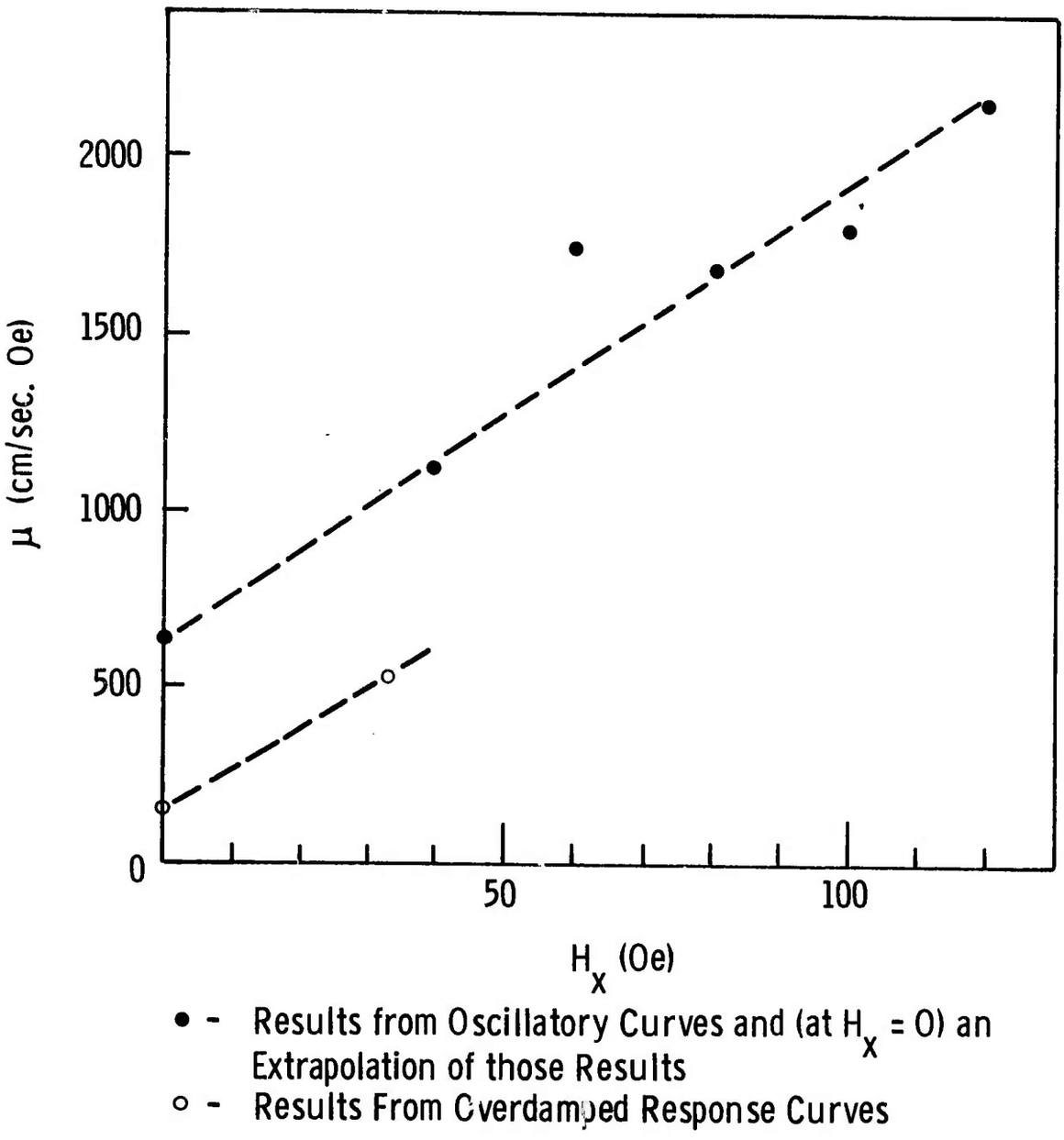

Figure 6. Domain Wall Mobility vs. In-Plane Field for a Typical Sample of Eu-Yb-Y Garnet

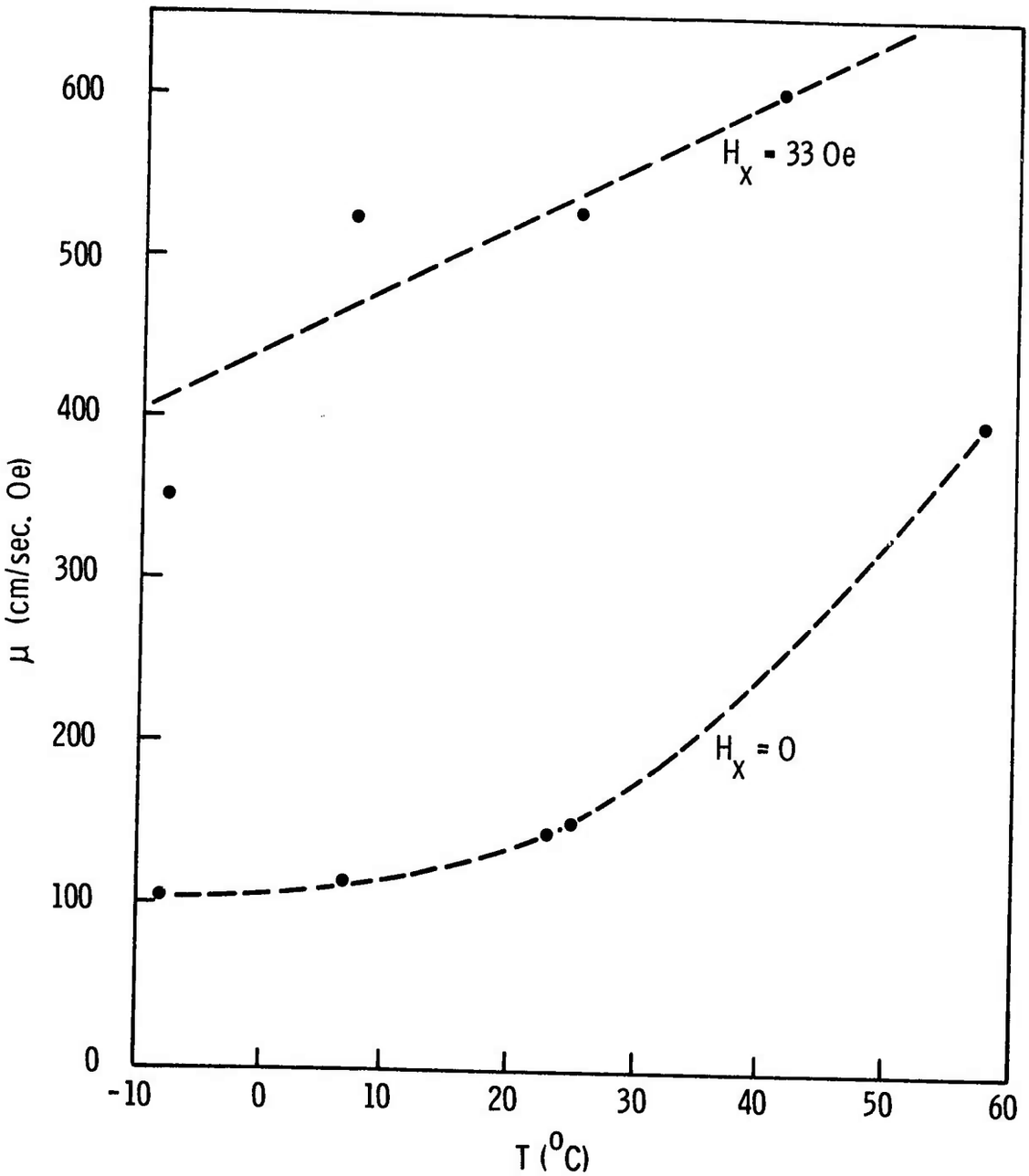

Figure 7. Domain Wall Mobility vs. Temperature in a Typical Sample of Eu-Yb-Y Garnet - All Results are Over-damped Response Curves

There are some interesting correlations between low coercivity and high mobility values within this system which should be further studied. Possibly both of these desirable properties are associated with the absence of a very small scale network of defects. Such a network, when present, might not only hold up domain walls, thereby increasing coercivity, but also cause the wall motion to be more turbulent and thus reduce mobility, perhaps through nucleation of in-plane Bloch lines.[17, 18] This network might arise at the film-substrate interface from a lattice mismatch of substrate and film too small to produce cracking.

3.4 The Sm-Y System

3.4.1 Introduction

It has been pointed out previously[2] that Sm ions are among those which are of interest as additions to $Y_3Fe_{5-x}Ga_xO_{12}$. $Sm_3Fe_5O_{12}$, like $Eu_3Fe_5O_{12}$, does not exhibit a compensation point. Hence, the magnetic properties of the mixed Sm-Y garnets are expected to exhibit good temperature stability. However, the damping parameter of the Sm ion is much higher than that of the Eu ion[14] and, therefore, might be expected to affect the intrinsic mobility of $Y_3Fe_{5-x}Ga_xO_{12}$ films to a greater extent than Eu ions. On the other hand, since some damping is required to reduce dynamic instabilities and to linearize the velocity-drive field relationship, mixed Sm-Y garnets (containing small amounts of Sm) might be expected to exhibit reasonable wall mobilities at practical drive fields. Therefore $Sm_yY_{3-y}Fe_{5-x}Ga_xO_{12}$ films were among those grown and supplied to the Sponsor.

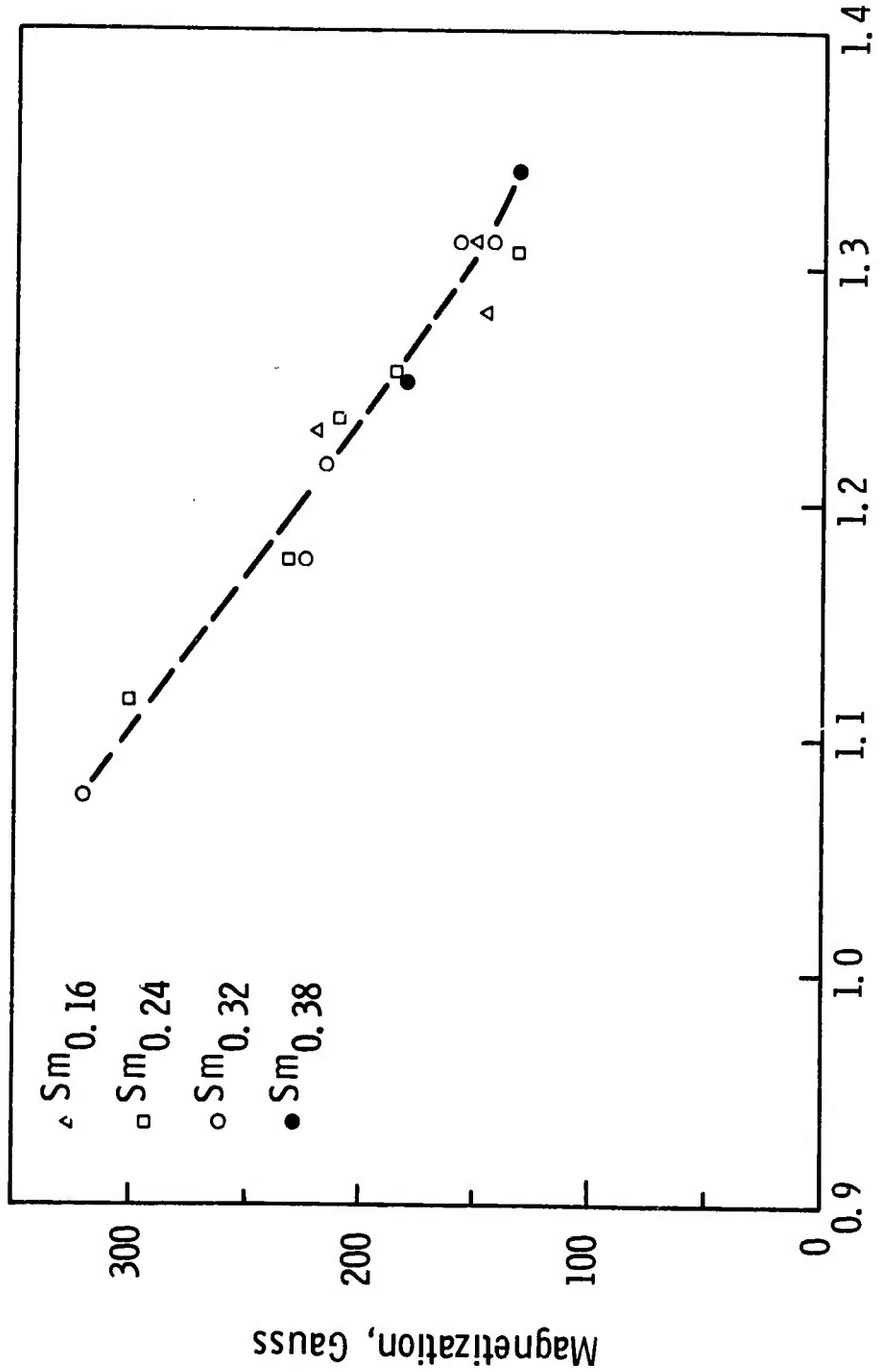

Figure 8. Magnetization vs. Gallium Content for Sm-Y Garnets

3.4.2 Properties of Sm-Y Garnet Films

3.4.2.1 Saturation Magnetization

In Fig. 8, room temperature saturation magnetization is plotted as a function of gallium content for films containing various concentration ratios of Sm/Y. Since the films are not of the same or optimum thickness, there is some scatter in the data. However, the general trend is obvious. Magnetization decreases with increasing Ga and does not depend strongly, if at all, on the concentration ratio of rare-earth ions.

3.4.2.2 Characteristic Length

The behavior of the characteristic length, ℓ, with composition is illustrated in Fig. 9. Again, the scatter in the data results from the films being of different thicknesses. Characteristic length is seen to be independent of Sm/Y concentration ratio.

Since the characteristic length of domains in films which support stable 6 μm bubbles is about 0.75 μm, a Ga content of about 1.3 ion/molecule is required.

3.4.2.3 Coercivity

Fig. 10 is a plot of coercivity vs Ga content of the various films. The coercivity is quite low and independent of Ga content for x less than about 1.2 ion/molecule. For higher x, it increases rapidly with Ga content. This behavior is believed to be related to the lattice mismatch between film and substrate. The films are grown in tension and lattice mismatch increases with increasing Ga. The rise in coercivity with Ga is believed to result from

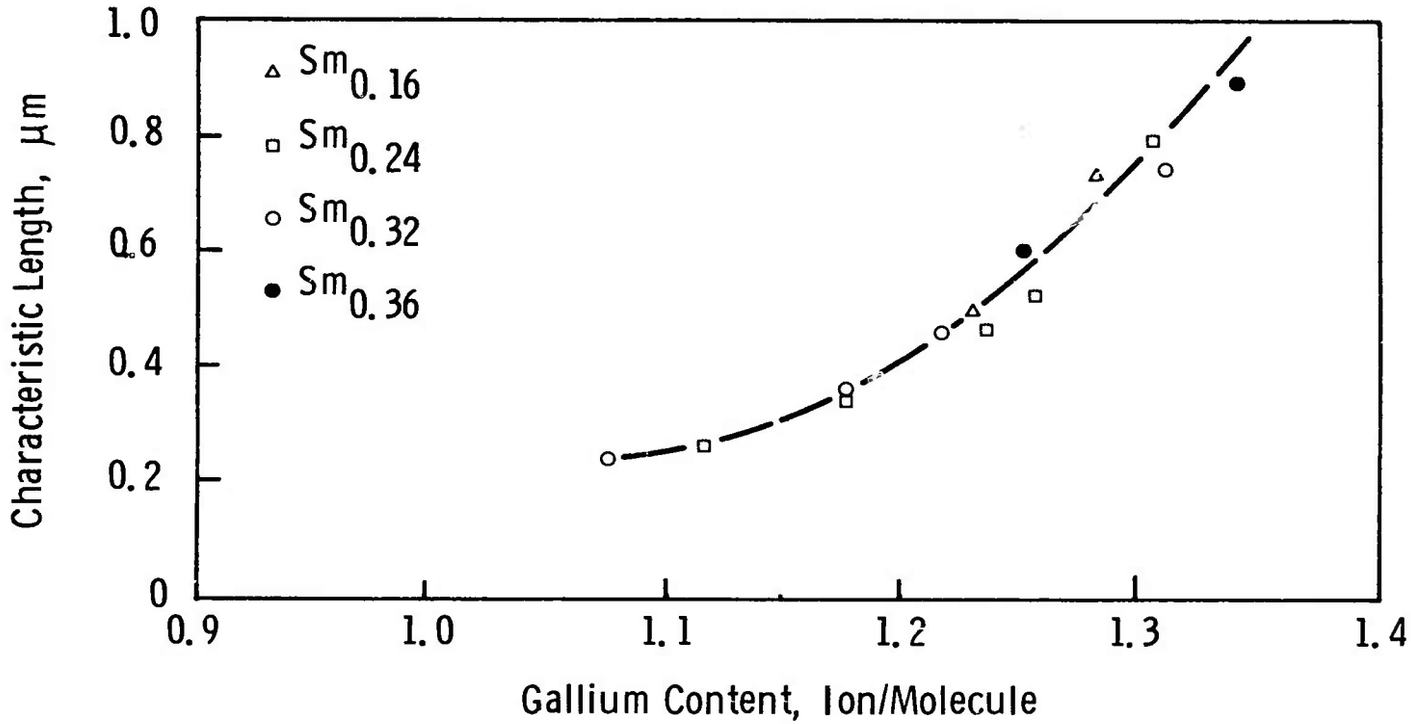

Figure 9. Characteristic Length vs. Gallium Content for Sm-Y Garnets

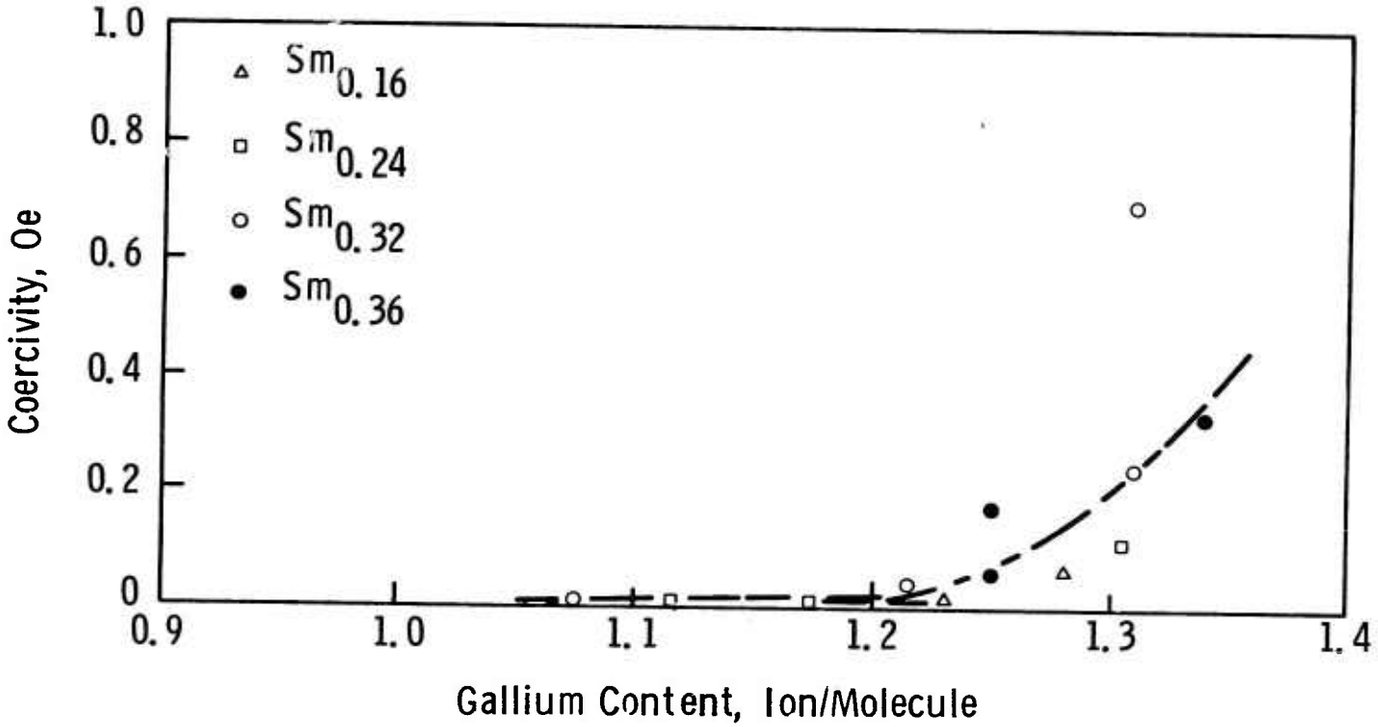

Figure 10. Coercivity vs. Gallium Content for Sm-Y Garnets

excessive mismatch. Since a Ga content of about 1.3 ion/molecule is required for stable 6 μm bubbles a good lattice match could be ensured with a Sm content of about 0.5 ion/molecule (based on Vegard's law).

3.4.2.4 Anisotropy

The anisotropy field and the anisotropy energy density for a number of films are given in Table 1. These films were grown at somewhat different temperatures and growth rates and since anisotropy is dependent on these growth conditions, the values are not strictly comparable. However, the values are illustrative of the magnitude of the anisotropy which can be obtained in this garnet system. The anisotropy field of films which support stable 6 μm bubbles is about 1500 Oe and the saturation magnetization is about 150 Gauss. These values result in a quality factor of about 10 for these films.

TABLE 1

Uniaxial Anisotropy of Some Sm-Y Films

Sample No.	Composition Sm	Composition Ga	Magnetization (Gauss)	Anisotropy Field (Oe)	Anisotropy Energy Density (erg/cm²)
5564A	0.16	1.23	220	970	8468
5565A	0.16	1.28	146	1480	17150
5567A	0.24	1.25	183	1220	8859
5571B	0.24	1.31	134	1440	7657
5577B	0.32	1.18	228	1210	10948
5578A	0.32	1.24	194	1540	11855
5586C	0.32	1.27	149	1500	8870
5562B	0.36	1.25	187	1770	13134
5562E	0.36	1.33	134	1685	8960

The data of Table 1 suggest that the anisotropy energy density decreases slightly with increasing Ga for a particular Sm/Y concentration ratio even though the anisotropy field appears to increase. This is probably a consequence of the rapid decrease of magnetization with Ga content (Fig. 8).

3.4.2.5 Mobility

Sm-Y films, when subjected to a step increase of bias field, always exhibit a simple wall motion to the final position (usually exponential) rather than an oscillatory motion. This is in keeping with the higher damping to be expected from Sm ions compared with Eu or Yb. There are additional problems present, however, which are presumably associated with the presence of Bloch lines in the domain walls. A typical sample which has been subjected to a variety of previous treatments will exhibit a characteristic response time (to 63% of final signal) of ~ 200 nsec. at $H_x = 0$. During this measurement the stripe domain pattern is observed to slowly move and change form. A similar slow response is often observed at $H_x = 40$ Oe. However, when the sample is subjected to a large in-plane field or a saturating bias field and then returned to $H_x = 40$ (not going through zero) a response approximately an order of magnitude faster is observed. In this condition the stripe pattern does not move visually. A reasonable explanation is that Bloch lines, originally in the walls, have been disposed of and the latter response is characteristic of walls free of Bloch lines. If H_x is now returned to zero one can often observe the pattern begin to move, first in an edge of the field of view and gradually spreading throughout as Bloch lines

spread through the pattern. One would expect that during this process a combination of the fast and slow responses might be seen. This has indeed been observed. In what follows emphasis is given to the faster response as that to be expected in a film in which hard bubbles have been suppressed (for example, by ion implantation).

The mobility values versus in-plane field are given for three compositions in Fig. 11. From the foregoing discussion it is clear that the values near $H_x = 0$ may be depressed by the presence of Bloch lines. However by $H_x = 40$ Oe this complication should be absent and, indeed, the data show the qualitative reduction of mobility to be expected as more of the highly damping Sm ion is introduced. Variability within a composition remains a problem with other samples of the $x = 0.32$ composition showing mobility at $H_x = 40$ as low as 180 cm/sec/Oe. It is clear, however, that quite useful mobilities are possible in this composition.

3.4.2.6 Temperature Coefficient of Characteristic Length

The characteristic length was measured as a function of temperature from about 0 to 50°C and the average temperature coefficient of characteristic length ($100 \Delta \ell / \ell \Delta T$) was calculated for that temperature range. The coefficient was about 0.5 percent/degree for all the compositions studied.

3.5 Nd-Y System

Epitaxial films of $Nd_yY_{3-y}Fe_{5-x}Ga_xO_{12}$ were deposited on (111) $Gd_3Ga_5O_{12}$ substrates. The nominal value of Nd ranged from 0.4 to 0.67 and x ranged from 1.0 to 1.2. The films were smooth and were not cracked.

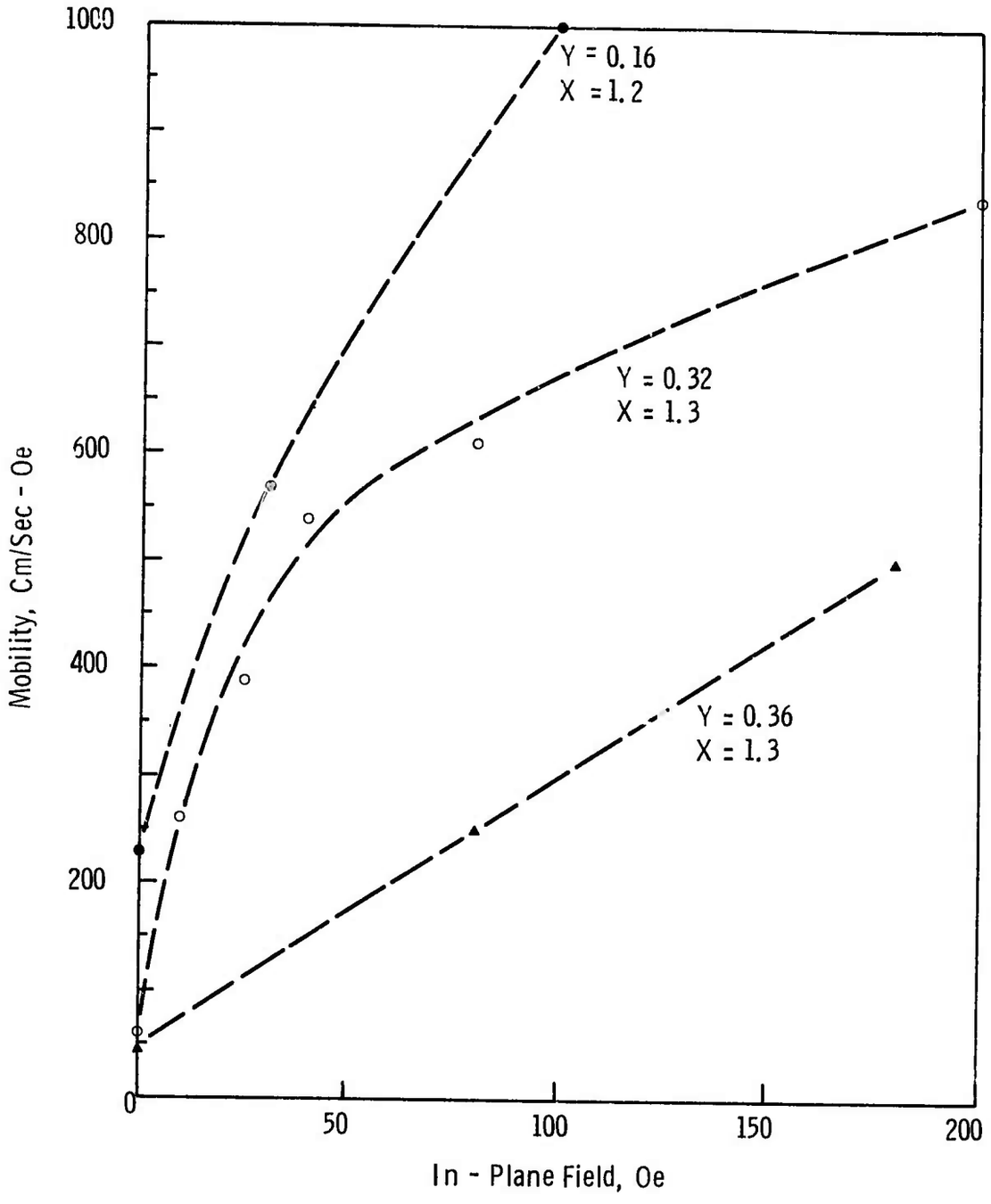

Figure 11. Mobility vs. In-Plane Field for Some $Sm_yY_{3-y}Fe_{5-x}Ga_xO_{12}$ Garnets

Thicknesses ranged from about 3 to 20 μm. The films did not exhibit uniaxial anisotropy in the <111> direction, the magnetization apparently lying in the plane in all cases. Anamolous anisotropy effects have also been noted in bulk, flux-grown, Nd-containing garnets by Gyorgy, et al.[19]

3.6 Discussion

Both the Eu-Yb-Y and Sm-Y systems appear to be promising candidates for bubble device application. The garnets exhibit reasonable mobilities, satisfactory quality factors and good temperature stability. Coercivity can be minimized by assuring a close lattice match between film and substrate. Compositions which support stable 5 - 7 μm bubbles have been identified.

Additional work with these systems could be quite rewarding. The relationship between mobility and composition is not entirely clear. In addition the proposed relationship between mobility and coercivity particularly apparent in the Eu-Yb-Y system deserves further study. Such a relationship could have an important bearing on bubble technology regardless of film composition. A detailed study might lead to a better understanding of wall mobility and wall turbulence in garnet films.

4.0 PLASMA SPRAYING

4.1 Introduction

Plasma spraying was investigated to determine its potential to produce magnetic garnet films of the composition $GdEr_2Fe_{4.5}Ga_{0.5}O_{12}$ with superior or unique properties, or to produce magnetic films with satisfactory characteristics at lower cost than traditional crystal growth processes.

Two approaches were designated for study: (1) the conversion of plasma-sprayed polycrystalline garnet films into monocrystalline films, and (2) the direct fabrication of plasma-sprayed monocrystalline garnet films. The first approach was a two-step process for forming monocrystalline films. It consisted of spraying polycrystalline films containing garnet and flux and subsequently converting the deposits into monocrystalline garnet films by a thermal treatment. Results of this work were reported in the Semi-Annual Technical Report.[2]

The second approach was a simplified process in which the film deposition and thermal treatment were performed in close order to reduce the operation to an essentially single step. This method was studied during the second portion of this contract and results of this work are reported in this section of the report.

4.1.1 Growth from the Melt

The first and most straight-forward approach at garnet film growth by direct deposition was growth from a melt. Garnet powder was fed slowly into the D.C. arc plasma torch and deposited as a molten film. This approach was unsuccessful due, primarily, to the temperature variations

experienced by the substrate during plasma spraying and the inability to maintain the stoichiometric composition of the incongruently melting garnet. Films deposited in this manner were essentially polycrystalline.

4.1.2 Growth from Solution

Other studies were made using a modified liquid epitaxy approach similar to the work performed during the first period of this contract, except that both plasma spray deposition and subsequent single crystal film growth were accomplished in the same apparatus without interim cooling to room temperature. The heated particulate was sprayed onto the substrate and formed a molten solution of flux and garnet on the substrate surface. Film growth was initiated by cooling the solution to a preselected growth temperature.

After several conversion runs were made using the D.C. plasma torch as both the means of powder deposition and the substrate heat source, an auxiliary resistance furnace was found to be a more stable and uniform high temperature heat source for film growth. Thereafter the D.C. plasma torch was used only as a means of providing heat to the powder for melting and deposition on the substrate.

The D.C. plasma heat source was abandoned in favor of the R.F. plasma source early in the program because of the latter's lower gas velocity and resulting gentler deposition of the molten particles. In addition, the absence of consumable electrodes in the R.F. plasma resulted in a cleaner film growth environment. As with the D.C. plasma, the use of an auxiliary heater during film growth provided a stable and uniform growth temperature.

The best bubble garnet films prepared during the second period of this program were grown using the R.F. plasma torch in conjunction with an auxiliary heater.

4.2 Experimental

4.2.1 R.F. Plasma Spraying

The radio-frequency (R.F.) plasma process used during most of this study was first proposed by T. B. Reed[20]. It represents an attractive way to heat a particulate to a high temperature without introducing electrode impurities. The overall process and equipment are shown schematically in Fig. 12.

Electrical power is supplied to a load coil by means of a 30-kW induction heating unit (Lepel, Model T-20-3-DF 1-E-H) having a resonance frequency of ~3.5 magacycles. The plasma acts as a 1-turn secondary coil to the 4-turn load coil. A shielded coaxial copper tube is used on the positive side of the R.F. coil to prevent energy loss.

The R.F. plasma is initiated by a high-voltage discharge produced with a Tesla coil. Once the argon gas is partially ionized, it couples efficiently with the R.F. field and sustains itself continuously as long as plasma-forming gas is supplied. In order to efficiently initiate a plasma, the impedance of the power unit and of the load coil must be properly matched. By so doing, the reflected power is substantially reduced.

The R.F. plasma torch (shown in detail in Fig. 13) consists of two concentric quartz tubes with three independent gas streams. Cooling air flows between the tubes to prevent melting. It is blocked from entering the hot zone by a graphite ring. Argon gas flows through the inner tube and forms

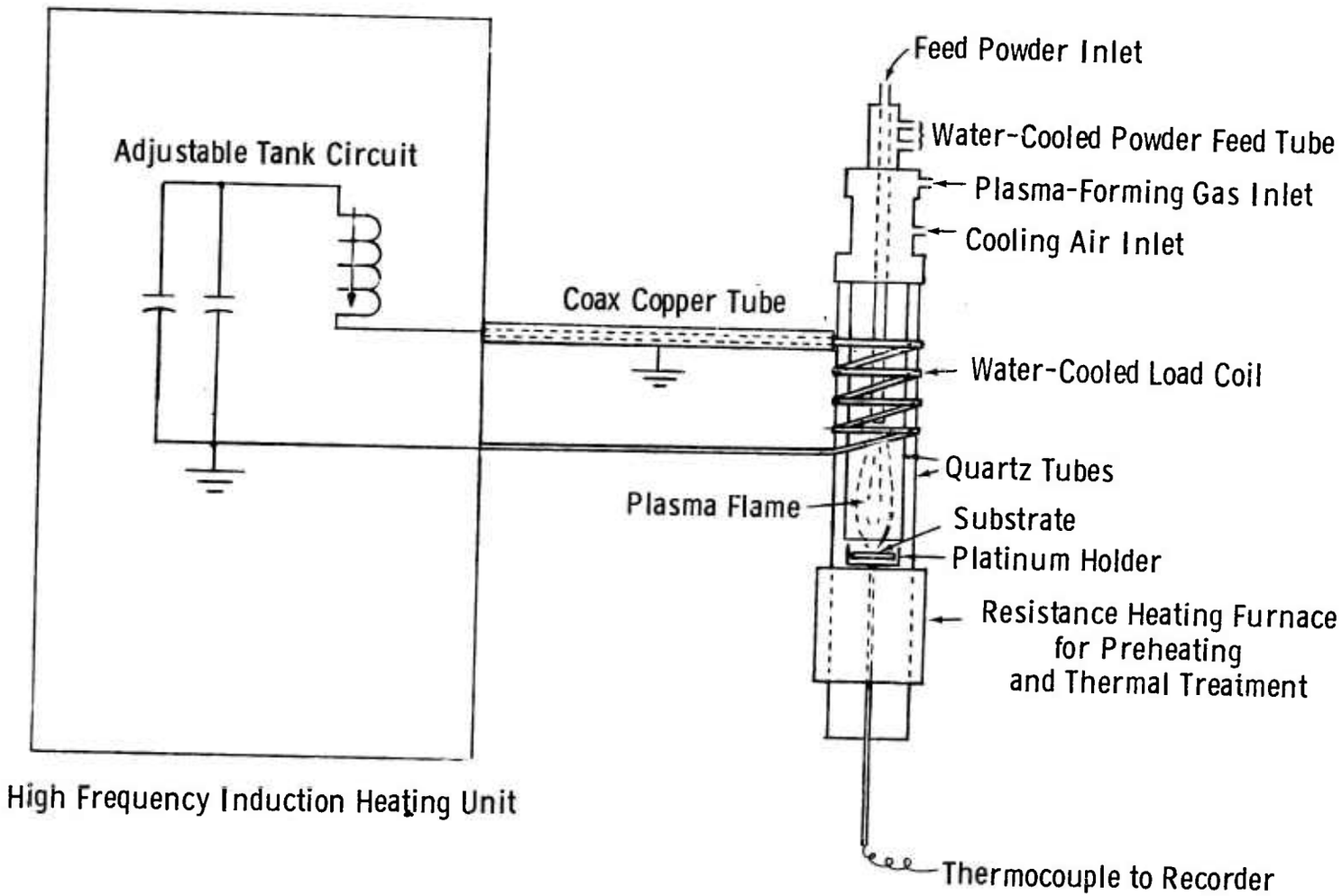

Figure 12. Schematic of R. F. Plasma Spraying Station

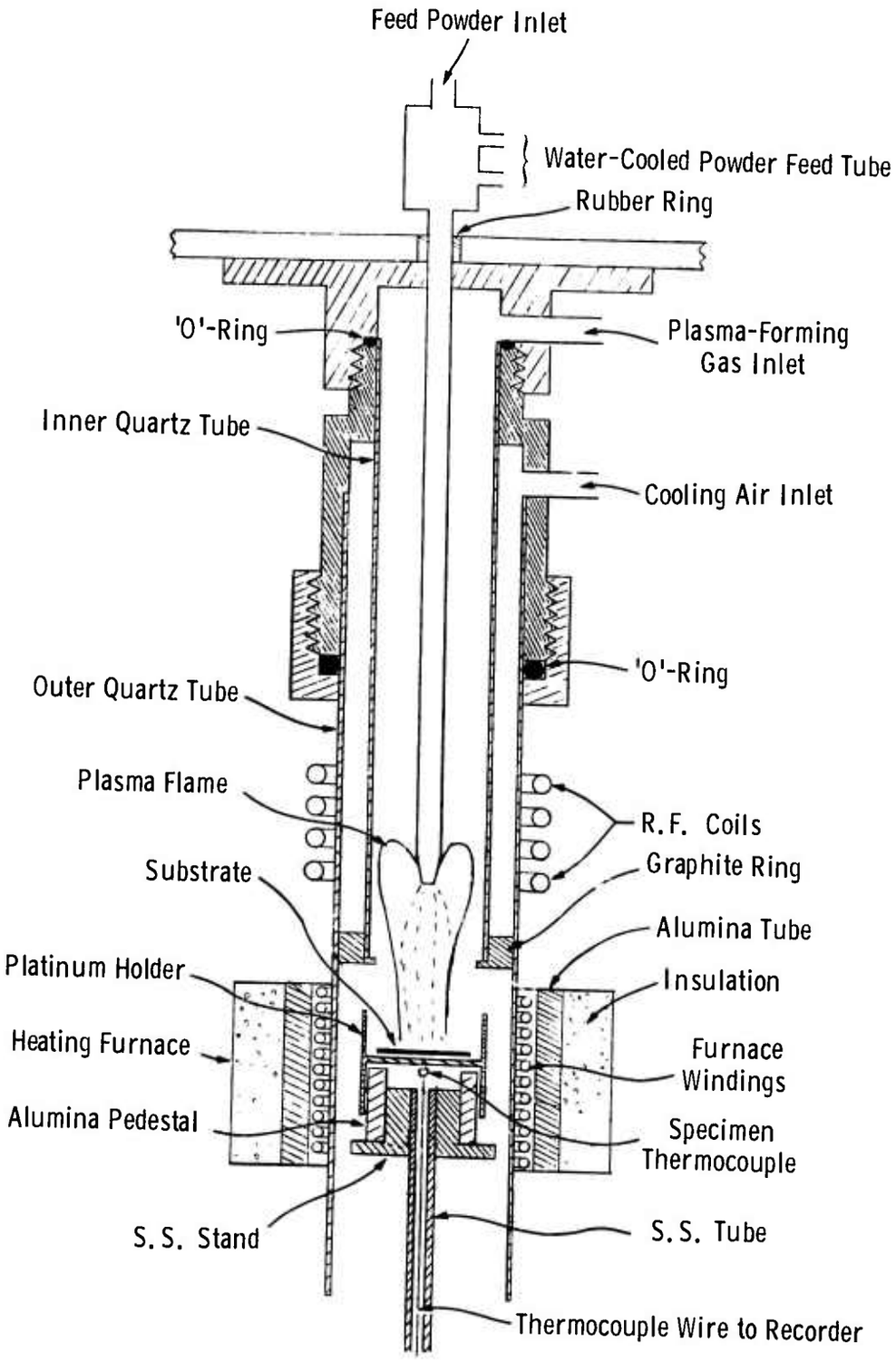

Figure 13. R. F. Plasma Torch Detail

the main body of the plasma. It is injected tangentially so as to create a vortex which forms a low pressure region in the center of the plasma. Circulation of some of the ionized gas up the center of the plasma provides enough seed gas to continuously maintain the plasma. Finally, oxygen gas, flowing through a water-cooled copper tube, carries powder through the high-temperature plasma for melting and deposition on the pre-heated substrate.

A cylindrical 4-turn R.F. coil of copper tubing surrounds the outer tube and serves to couple energy into the plasma. To provide a uniform preheat and growth temperature over the substrate, an auxiliary furnace is fitted around the outer quartz tube below the induction coil.

After preheating the GGG substrate to a specific temperature in the auxiliary furnace, the substrate is quickly removed from the furnace and positioned at the appropriate distance from the powder tube outlet. Powder is transported from a feeder using an oxygen carrier gas and passed through the high-temperature region for heating in the plasma stream. Powder is thus melted in the plasma flame and deposited on the substrate. The substrate temperature is monitored continuously using a Pt. Pt - 13% Rh reference-grade thermocouple which is in physical contact with the bottom of the platinum substrate holder. After deposition, the sprayed substrate is quickly returned to the furnace for film growth and held for a specific time. Once film growth is terminated, the flux is decanted from the surface and residual flux is then removed using a dilute solution of HNO_3.

4.2.2 D.C. Plasma Spraying Station

Initial experiments to fabricate bubble garnet films by spraying without cooling to room temperature and subsequently reheating to form the epitaxial film were made using the D C. arc plasma torch discussed in the Semi-Annual report.(2)

The D. C. plasma spraying station is shown in Fig. 14. The plasma torch is mounted against a metal bellows which allows movement of the spray torch to permit uniform coverage while minimizing contamination from circulating air during the powder deposition. A quartz tube is placed against the bottom of the bellows to act as an enclosure for the substrate during spray deposition and film growth. The auxiliary furnace is placed around the quartz tube to provide a uniform growth temperature across the substrate. Once the substrate has reached the preheat temperature, the plasma torch is activated and powder is injected through the plasma. The molten particulate then collects on the substrate and the specimen is held at the growth temperature for a specific time as required to form an epitaxial garnet film. After growth, excess flux present is removed in a dilute solution of HNO_3.

4.2.3 Material

Gadolinium oxide (Gd_2O_3), erbium oxide (Er_2O_3), and boron oxide (B_2O_3) were obtained from Research Inorganic/Organic Corporation and were 99.9%, 99.9%, and 99.99% pure, respectively. Grade I iron oxide (Fe_2O_3), gallium oxide (Ga_2O_3) and lead oxide (PbO) manufactured by Johnson Matthay Chemicals Limited, were obtained from United Mineral and Chemical Corporation, each having a purity of 99.99%.

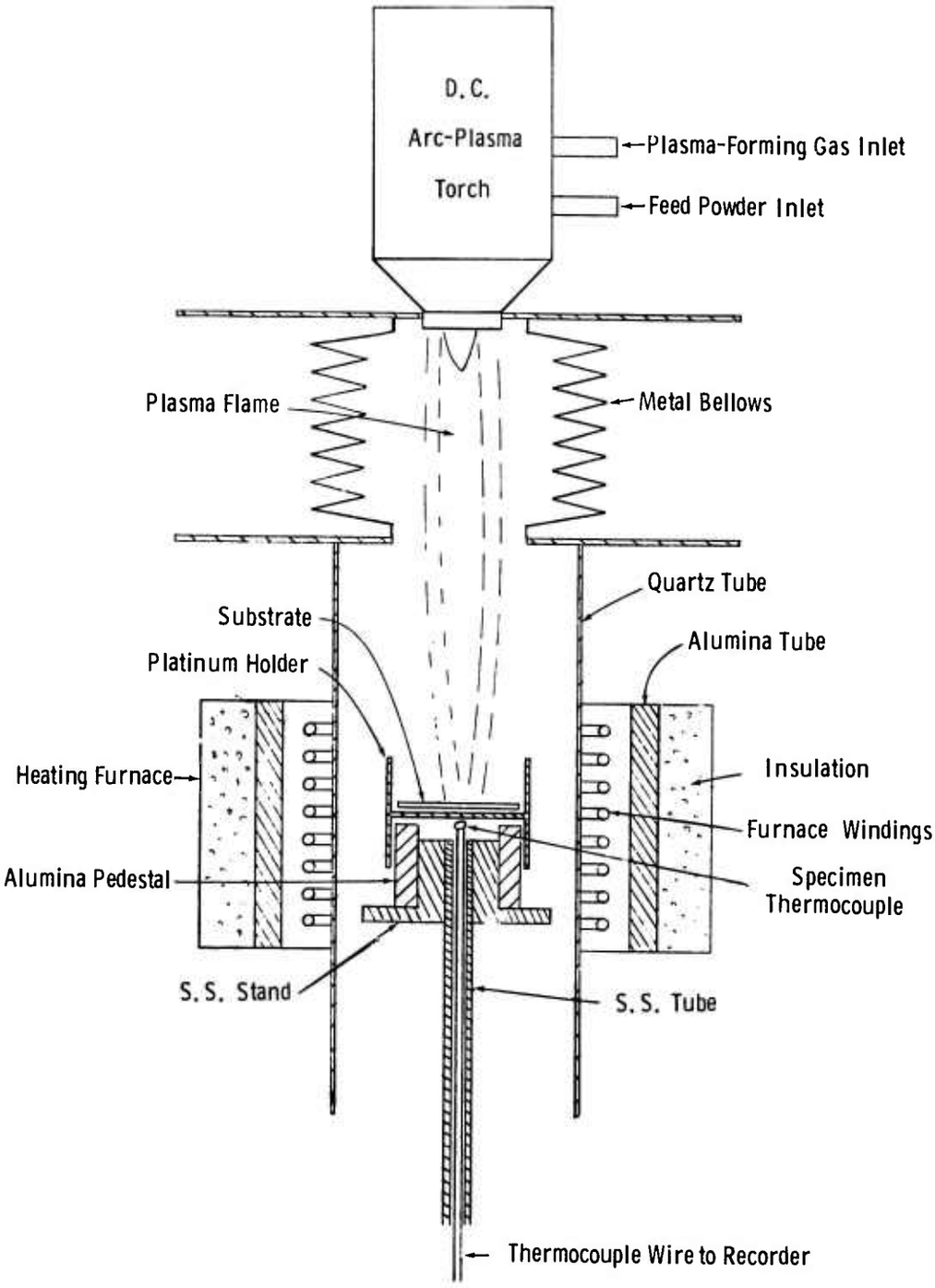

Figure 14. D. C. Plasma Spraying Station

The individual oxides were weighed to four significant figures using an Ainsworth triple beam balance. The oxides were combined to form the mixture shown in Table 2 and then blended for one hour.

The blended oxides were placed in a platinum boat and heated for 2 hours at 1300°C in air. The sintered charge was then pulverized into a fine powder which after sifting, was suitable for injection into the plasma torch and used in studies to determine the feasibility of producing epitaxial garnet films directly from the melt.

A homogeneous mixture of the oxides in the garnet and flux powder was obtained by forming a solution at high temperature. The solution was heated in a closed platinum crucible at ~ 1100°C for 2 hours and then quickly poured into a platinum boat. The resultant ingot was pulverized using a mill containing a tungsten carbide rotating blade to form a powder which, after sifting, was suitable for injection into the plasma spray torch for producing films from solutions.

The < 111 > GGG substrates (~ 14 mils thick) were all obtained with one side polished. Some substrates (~ 3/4" diameter) were scribed on the unpolished side and broken into quarters in order to conserve substrate material. Other (~ 1/2" diameter) substrates were used as received. The substrate cleaning procedure prior to spraying has been described previously.[2]

4.3 Results and Discussion

As in the first portion of this contract, the approximate composition $GdEr_2Fe_{4.5}Ga_{0.5}O_{12}$ was studied. This garnet exhibits growth-induced

TABLE 2

Powder Compositions

Garnet Powder for Growth from the Melt	
Component	Weight%
Gd_2O_3	4.49
Fe_2O_3	77.66
Er_2O_3	13.05
Ga_2O_3	4.80

Garnet & Flux Powder for Growth from Solution	
Component	Weight%
PbO	91.26
B_2O_3	1.83
Gd_2O_3	0.31
Fe_2O_3	5.37
Er_2O_3	0.90
Ga_2O_3	0.33

anisotropy perpendicular to the film plane. A good lattice constant match is obtained between this garnet and <111> GGG substrate.

4.3.1 D.C. Plasma Spraying

4.3.1.1 Epitaxial Crystal Growth from the Melt

Efforts to form single crystal garnet films directly from the melt were largely unsuccessful. Powder sprayed using the D.C. plasma torch was slowly deposited on GGG substrates, maintained at 1200 - 1300°C, and then slowly cooled to room temperature. However, the resultant deposits were essentially polycrystalline. This was attributed to temperature non-uniformity and temperature fluctuation within the substrate during spraying.

4.3.1.2 Epitaxial Crystal Growth from Solution

Magnetic garnet film growth was achieved by using the D.C. plasma torch for depositing a film of garnet and flux on a preheated substrate and subsequently maintaining the specimen at the film growth temperature for several minutes. However, domains were observed only in isolated areas of the film after conversion and the results were not reproducible. Typical conditions used for producing a garnet film by D.C. arc plasma spraying are shown in Table 3.

In general, the films produced by D.C. arc plasma spraying were inferior to those produced by the R.F. plasma spraying method. The high kinetic energy imparted to the injected particulate caused the molten flux and garnet to flow off the substrate during deposition. Consequently, only a portion of the sprayed solution was available for growing an epitaxial film on the GGG substrate.

TABLE 3

Typical Conditions for Growing Epitaxial Garnet Films from a Flux Using D.C. Arc Plasma Spraying

Spray Torch	Plasmadyne Model SG-3 (25 kW)
Arc Gas	Argon at 50 cfh
Arc Current	250 amps
Powder Feed Mechanism	
Type	Plasmadyne Rotofeeder
Carrier Gas	Oxygen at 15 cfh
Growth Conditions	
Substrate Preheat Temp.	930°C
Growth Temperature	930°C
Growth Time	10 minutes

4.3.2 R.F. Plasma Spraying

The R.F. plasma method of growing bulk single crystal oxides was successfully demonstrated by Reed.[21] However, the oxides in his work were simple congruent melting compounds in which bulk crystals were grown directly from the melt. The difficulty in maintaining the correct composition of the bubble garnet from the melt made growth from a solution more attractive. However, garnet films made from a solution were inferior in overall quality as compared to films made by liquid epitaxy using the "dip process."

The R.F. plasma method has several drawbacks when compared to the liquid phase epitaxy method. First, the temperature uniformity across the substrate obtainable by the "dip process" is difficult to achieve using an R.F. plasma. Temperatures vary from the center of the plasma to the boundary causing composition and film thickness variations in films grown by R.F. plasma.

High defect density can probably also be attributed to the plasma process. This conclusion is based on a liquid epitaxy "dip" experiment using garnet-flux prepared by melting the powder employed in R.F. plasma growth studies. In addition, GGG substrates were prepared in the manner typically used for spraying studies. The time-temperature conditions previously found satisfactory for film growth by the "dip" process were used. Nearly defect-free films were grown indicating that substrate and powder preparation procedures were satisfactory. Apparently, the exposed surface of the GGG substrate during and before plasma spraying was vulnerable to

airborne contaminants. Also, the long exposure time of the substrate to the flux probably contributed to the high defect density.

Finally, it was difficult to maintain the sprayed solutions in the garnet stability range. The films were invariably contaminated with crystallites of orthoferrite, hematite or other phases.

4.3.3 Characteristics of Selected Garnet Films

All films produced in this program were qualitatively examined using an optical microscope to determine defect density and overall film quality. Domain patterns were observed using polarized light. Film color was macroscopically noted.

None of the garnet films made by D.C. plasma spraying from the melt exhibited magnetic domains. However, films primarily sprayed from solution did display domains over small isolated areas.

During the second phase of this program, 47 garnet films were deposited on GGG substrates using the R.F. plasma spraying method. In general, domains were observed in most of the films. Defect density was usually high and the surface of such films was uneven or faceted.

Five selected garnet films representative of the direct fabrication method using the R.F. plasma were further characterized and the results are summarized in Table 4. The spray process conditions used in growing these epitaxial films from the flux are shown in Table 5. In all samples, the variation in film thickness and the high defect density made magnetic characterization difficult using conventional techniques.

Sample films representative of the results obtained by the spraying process were delivered to the Sponsor.

TABLE 4

Characterization Data of Selected Bubble Films Made by the Method of R.F. Plasma Spraying

Sampler Number	R.F. Run No.	h	ℓ	$4\pi M_s$	H_c	H_s-b	ds-b	H_0	d_0	δ_w	Percent of Film Area Containing Domains	Defects	Film Color
APS 6	15	2.86	.86	138	.93	24	8	39	5	.13	40	Few	Orange
APS 7	16	-	-	-	-	-	-	-	-	-	40	Many	Orange-Yellow
APS 8	18	-	-	-	-	-	-	-	-	-	80	Few	Orange-Yellow
APS 9	24	-	-	-	-	-	-	-	-	-	75	Very Few	Orange-Yellow
APS 10	25	-	-	-	-	-	-	-	-	-	75	Few	Orange-Yellow

Legend:

h	Film thickness	μm	ds-b	Bubble diameter at Hs-b	μm
ℓ	Characteristic length	μm	H_0	Bubble collapse field	Oe
$4\pi M_s$	Saturation Magnetization	Gauss	d_0	Bubble diameter at H_0	μm
Hc	Coercivity	Oe	δ_w	Domain wall energy/unit area	ergs/cm^2
Hs-b	Strip to Bubble transition field	Oe			

TABLE 5

Process Conditions Used for Preparing

Selected Representative Films by the Method of

R.F. Plasma Spraying

Sample Number	R.F.* Run No.	RF Power Level, kW	Plasma Gas Type	Plasma Gas Flow, cfh	Powder Gas Type	Powder Gas Flow, cfh	Substrate Preheat Temp., °C	Substrate Avg. Spraying Temp., °C	Spray Time min.	Films Growth Temp., °C	Films Growth Time, min.
APS 6	15	4.06	Argon	200	Oxygen	10	950	1000	2.3	935	29
APS 7	16	3.42	Argon	200	Oxygen	10	930	950	3.5	930	24
APS 8	18	3.36	Argon	200	Oxygen	10	950	920	5.0	940	15
APS 9	24	3.36	Argon	200	Oxygen	10	980	1150	3.5	937	24
APS 10	25	2.75	Argon	300	Oxygen	10	910	1125	1.7	935	15

5.0 BULK CRYSTAL GROWTH

At the beginning of this program $Gd_3Ga_5O_{12}$ substrates of 15-18 mm diameter were available commercially. Although the dislocation and inclusion densities were acceptable the crystals contained an undesirable, highly strained central core. The lattice parameter of the core was found to be 0.001 - 0.002Å larger than the surrounding region. The Czochralski growth of $Gd_3Ga_5O_{12}$ developed rapidly during this program and now nearly perfect, core-free crystals of up to 38 mm in diameter are available. Lattice parameter variations within the crystal of less than 0.0005Å can be maintained. There appears to be no inherent reason why even larger crystals of the same quality cannot be grown.

The conditions required to grow high quality, core-free gallium garnet crystals have been adequately discussed in previous reports[1, 2] and will not be detailed here. The optimum rotation and growth rates for crystal growh were found to depend on the amount of furnace insulation, thermal gradients within the furnace, and the relative diameter of the crystal and crucible. Hence, the "optimum"conditions are peculiar to a particular furnace arrangement and it is not possible to specify rotation and pull rates that can be used in general. These conditions must be determined empirically for each furnace arrangement.

During the second period of this contract, high quality single crystal of $Gd_3Ga_5O_{12}$ were grown routinely to supply substrates for epitaxial films.

6.0 CONCLUSIONS AND RECOMMENDATIONS

The technology of garnet bubble materials has advanced rapidly during the last two years. This is due in great part to the development of LPE growth of garnet films. Levinstein, et al.,[11] discovered the remarkable stability of supercooled solutions of garnet in $PbO-B_2O_3$ and first described the simple "dipping" method of film growth. Since then, the technique has been used extensively in the preparation of multicomponent, uniaxial garnet films. This is the method used to prepare the high quality films supplied the Sponsor during this project.

Most of the garnet LPE work has been done in PbO-based solvents. However, Linares[22] investigated other solvents including those based on BaO. Recently, the BaO-based solvent has been the subject of an intensive investigation by workers at Hewlett-Packard Laboratories.[23] This solvent was also investigated in this work.[1] The BaO-based solvent exhibits several desirable features including low volatility, non-corrosiveness and low toxicity. However, the high viscosity of the melt at practical film growth temperatures and the attendant difficulties of solvent drainage from the film have been serious deterrents to its widespread use.

Epitaxial garnet films have been prepared by methods other than LPE, including CVD, APS, sputtering and coprecipitation/annealing. The CVD and APS processes have been studied as a part of this project. High quality films can be prepared by CVD but it is extremely difficult to achieve run-to-run reproducibility with the complex garnet films of interest to present day bubble technology. Most workers in the field have now abandoned the CVD approach.

In respect to APS, the major problem appears to be control of phase relationships. Epitaxial garnet films grown by APS are usually contaminated with crystallites of orthoferrite, hematite, magnetoplumbite and/or other solid phases. Low defect density films have not been grown and the elimination of unwanted phases appears to be a formidable problem.

An understanding of the mechanics and kinetics of LPE film growth has been developed[24, 25] and the reproducibility of the process has been demonstrated.[26] All recent developments indicate that LPE "dipping" growth of garnet films is a commercially viable process. Remarkable progress has been made in the relatively short time the process has been used to grow magnetic garnet films. It is reasonable to expect that additional progress will be made in the future. It is believed that nearly all workers in this field are now using the LPE "dipping" method and this situation is expected to continue.

The growth of bulk, non-magnetic garnet crystals for substrates has kept pace with the development of epitaxial film growth. Core-free single crystals with dislocation densities less than 5 per cm^2 can be readily grown by the Czochralski technique. Such crystals, up to 38 mm in diameter, are now available from commercial vendors.

A number of film compositions were delivered to the Sponsor during this project. These films, tailored to support 5 - 7 μm bubbles, represented a variety of bubble materials. Included were films of primarily stress-induced anisotropy, primarily growth induced anisotropy and films in which

both growth and stress-induced mechanisms were important. At least two garnet systems, Eu-Yb-Y, and Sm-Y were identified as being of particular practical interest. These garnets exhibit reasonable mobilities, satisfactory quality factors and good temperature stability.

The "hard" bubble problem was not recognized when this project was initiated and has not been a subject of this work. However, two different, more or less successful solutions have been developed by others. These are (1) the epitaxial deposition of a "capping" layer[27] and (2) ion-implantation.[28]

Although a good understanding of garnet bubble films has been obtained to date, additional work is needed. In particular, it is felt that detailed study of the possible relationship between wall mobility and turbulence and coercivity might be especially rewarding.

7.0 REFERENCES

1. J. W. Moody, R. M. Sandfort, and R. W. Shaw, Final Report, Magnetic Bubble Materials, MRC-SL-341, Contract No. DAAH01-72-C-0490, August 11, 1972.

2. J. W. Moody, R. M. Sandfort, R. W. Shaw, and R. J. Janoweicki, Semi-Annual Technical Report, Magnetic Bubble Materials MRC-SL-354, Contract No. DAAH01-72-C-1098, Feb. 11, 1973.

3. R. W. Shaw, R. M. Sandfort, and J. W. Moody, Magnetic Bubble Materials: Initial Characterization Report, MRC-SL-326, Contract No. DAAH01-72-C-0490, March, 1972

4. R. W. Shaw, R. M. Sandfort, and J. W. Moody, Magnetic Bubble Materials: Characterization Techniques Study Report, MRC-SL-339, Contract No. DAAH01-72-C-0490, July, 1972

5. D. C. Fowlis and J. A. Copeland, "Rapid Method for Determining the Magnetization and Intrinsic Length of Magnetic Bubble Domain Materials", AIP Conference Proceedings, No. 5, 240 (1971).

6. R. W. Shaw, D. E. Hill, R. M. Sandfort, and J. W. Moody, "Determination of Magnetic Bubble Film Parameters from Strip Domain Measurements", J. Appl. Phys., 44, 2346 (1973).

7. A. A. Thiele, "Theory of the Static Stability of Cylindrical Domains in Uniaxial Platelets", J. Appl. Phys., 41, 1139, (1970).

8. P. W. Shumate, Jr., D. H. Smith and B. F. Hagedorn, "The Temperature Dependence of the Anisotropy and Coercivity in Epitaxial Films of Mixed Rare-Earth Iron Garnets", J. Appl. Phys., 44, 449 (1973).

9. P. W. Shumate, Jr., "Extension of the Analysis for an Optical Mangetometer to Include Cubic Anisotropy in Detail", J. Appl. Phys., 44, 3323 (1973).

10. R. M. Josephs, "Characterization of the Magnetic Behavior of Bubble Domains", AIP Conference Proceedings, No. 10, 286 (1973).

11. H. J. Levinstein, S. Licht, R. W. Landorf, and S. L. Blank, "Growth of High Quality Garnet Thin Films from Supercooled Melts", Appl. Phys. Letters, 19, 486 (1971).

12. W. A. Bonner, J. E. Geusic, D. H. Smith, F. C. Rossol, L. G. Van Uitert, and G. P. Vella-Coleiro, "Characteristics of Temperature-Stable Eu-Based Garnet Films for Magnetic Bubble Application", J. Appl. Phys. 43, 3226 (1972).

13. NASA Contract No. NAS1-11794

14. G. P. Vella-Coleiro, "Domain Wall Mobility in Epitaxial Garnet Films", AIP Conference Proceedings, No. 10, 425 (1973).

15. Jerry W. Moody, Roger W. Shaw, and Robert M. Sandfort, and R. L. Stermer, "Properties of $Gd_yY_{3-y}Fe_{5-x}Ga_xO_{12}$ Films Grown by Liquid Phase Epitaxy", Intermag 1973, Proc., to be published.

16. B. E. Argyle and A. P. Malozemoff, "Experimental Study of Domain Wall Response to Sinusoidal and Pulsed Fields", AIP Conference Proceedings No. 5, 115 (1972).

17. J. C. Slonczewski, "Theory of Domain Wall Motion in Mangetic Films and Platelets," J. Appl. Phys. 44, 1759 (1973).

18. E. Schloemann, "Light and Heavy Domain Walls in Bubble Films", AIP Conference Proceedings, No. 10, 478 (1973).

19. E. M. Gyorgy, M. D. Sturge, L. G. Van Uitert, E. J. Heiler, and W. H. Grodkiewicz, "Growth Induced Anisotropy of Some Mixed Rare-earth Iron Garnets", J. Appl. Phys. 44, 438 (1973).

20. T. B. Reed, "Induction-Coupled Plasma Torch", J. Appl. Phys., 32. 821 (1961).

21. T. B. Reed, "Growth of Refractory Crystals Using the Induction Plasma Torch", J. Appl. Phys. 32 , 2534 (1961).

22. R. C. Linares, "Epitaxial Growth of Narrow Linewidth Yttrium Iron Garnet Films", J. Cryst. Growth, 34, 443 (1968).

23. see, for example, R. Hiskes and R. A. Burmeister, "Properties of Rare-Earth Iron Garnets Grown in BaO-Based and PbO-Based Solvents", AIP Conference Proceedings, No. 10, 304 (1973).

24. R. Ghez, and E. A. Giess, "Liquid Phase Epitaxial Growth Kinetics of Magnetic Garnet Films Grown by Isothermal Dipping with Axial Rotation", Mat. Res. Bull, 8, 31 (1973).

25. S. L. Blank, B. S. Hewitt, L. K. Shick, and J. W. Nielsen, "Kinetics of LPE Growth and Its Influence on Magnetic Properties", AIP Conference Proceedings, No. 10, 256 (1973).

26. B. S. Hewitt, R. D. Pierce, S. L. Blank and S. Knight, "Technique for Controlling the Properties of Magnetic Garnet Films", Intermag Conference, Washington D.C., 1973, to be published.

27. A. H. Bobeck, S. L. Blank, and H. J. Levinstein, "Multilayer Epitaxial Garnet Films for Magnetic Bubble Devices - Hard Bubble Suppression" Bell System Tech. J., 51, 1431 (1972).

28. R. Wolfe and J. C. North, "Suppression of Hard Bubbles in Magnetic Garnet Films by Ion Implantation", Bell System Tech. J., 51, 1436 (1972).

8.0 APPENDIX

8.1 Growth Parameters for $Eu_{0.5}Yb_{0.15}Y_{2.35}Fe_{3.8}Ga_{1.2}O_{12}$

Solution Composition:

Compound	Wt	Moles	Mol %
PbO	400.0	1.792	85.37
B_2O_3	8.000	0.1149	5.474
Eu_2O_3	0.7374	0.002095	0.09980
Yb_2O_3	0.2477	0.0006285	0.02994
Y_2O_3	2.2237	0.009846	0.4691
Fe_2O_3	25.2933	0.1584	7.546
Ga_2O_3	4.0491	0.02160	1.029
TOTAL	440.6	2.099	100.0

Liquidus Temperature: 976 C
Growth Temperature: 970 C
Rotation Rate: 200 rpm

8.2 Growth Parameters for $Sm_{0.36}Y_{2.64}Fe_{3.7}Ga_{1.3}O_{12}$

Solution Composition:

Compound	Wt	Moles	Mol %
PbO	400.0	1.7920	85.95
B_2O_3	8.000	0.1149	5.511
Sm_2O_3	0.6293	0.001804	0.08652
Y_2O_3	2.6482	0.01173	0.5626
Fe_2O_3	22.8199	0.1429	6.854
Ga_2O_3	4.0030	0.02136	1.024
TOTAL	438.1	2.085	100.0

Liquidus Temperature: 977 C
Growth Temperature: 970 C
Rotation Rate: 200 rpm